Cross-Layer Optimization and Receiver Localization for Cognitive Networks Using Interference Tweets

Antonio G. Marques, Emiliano Dall'Anese, and Georgios B. Giannakis

Abstract

A cross-layer resource allocation scheme for underlay multi-hop cognitive radio networks is formulated, in the presence of *uncertain* propagation gains *and* locations of primary users (PUs). Secondary network design variables are optimized under long-term probability-of-interference constraints, by exploiting channel statistics and maps that pinpoint areas where PU receivers are likely to reside. These maps are tracked using a Bayesian approach, based on 1-bit messages - here refereed to as "interference tweet" - broadcasted by the PU system whenever a communication disruption occurs due to interference. Although nonconvex, the problem has zero duality gap, and it is optimally solved using a Lagrangian dual approach. Numerical experiments demonstrate the ability of the proposed scheme to localize PU receivers, as well as the performance gains enabled by this minimal primary-secondary interplay.

Index Terms

Wireless cognitive radio networks, cross-layer optimization, receiver localization, Lagrange dual, Bayesian estimation.

IEEE Journal on Selected Areas on Communications: Cognitive Radio Series.

Submitted: March 27, 2013

This work was supported by the QNRF grant NPRP 09-341-2-128. A. G. Marques is with the Dep. of Signal Theory and Communications, Universidad Rey Juan Carlos, Camino del Molino s/n, Fuenlabrada, Madrid 28943, Spain. E. Dall'Anese and G. B. Giannakis are with the Digital Technology Center and the Dept. of ECE, University of Minnesota, 200 Union Street SE, Minneapolis, MN 55455, USA. E-mails: antonio.garcia.marques@urjc.es, {emiliano, georgios}@umn.edu. Part of this work was submitted to the *38th IEEE Intl. Conf. on Acoustics, Speech and Signal Processing*, Vancouver, Canada, May 2013, and to the *14th IEEE Intl. Workshops on Sig. Proc. Advances for Wireless Commun*, Darmstadt, Germany, June 2013.

I. INTRODUCTION

In an hierarchical spectrum access mode, underlay cognitive radios (CRs) can opportunistically (re-)use the frequency bands licensed to a primary user (PU) system, provided ongoing primary communications are not overly disrupted [1]. Once spectral opportunities are identified through sensing, control of the interference inflicted to incumbent users is crucial to enable a seamless coexistence of primary and CR-empowered secondary systems [2]–[5].

As in conventional wireless networking, knowledge of the propagation gains is instrumental to controlling the co-channel interference. However, since the PU system has generally no incentive to exchange synchronization and channel training signals with secondary users (SUs), SU-to-PU channels are difficult to acquire in practice. In lieu of instantaneous propagation gains, the *distribution* of the PU-to-SU channels can be used to limit the instantaneous interference inflicted to PUs by means of average or probabilistic constraints [2]–[10]. Power control for underlay CRs under channel uncertainty was considered in, e.g., [2], [3], for one PU link and one SU link. Instantaneous and average interference constraints were compared in [4] for the same setup, while an extension to multiple SU links can be found in e.g., [6]–[9].

State-of-the-art spectrum sensing schemes can detect and localize active PU *sources* [11]–[13], but not "passive" PU *receivers*, which may remain silent most of the time. Since localization based on received signal strength (RSS) measurements over (short) primary signalling messages such as e.g., (re)transmissions requests, is challenging (and these messages may be exchanged over a primary control channel), knowledge of the PU receiver locations must be assumed uncertain. A prudent alternative to bypass the need to gather information about the PU receivers' locations is to estimate the PU coverage region [11], [13], and ensure that the interference does not exceed a prescribed level at any point of the coverage region boundary [10], [13], [14]. However, this conservative approach leads to a sub-optimal operation of the SU network, especially when PU receivers are not close to the boundary. The alternative is to account for the uncertainty in the receivers location, which indirectly generates uncertainty on the gains of the SU-to-PU channels. This calls for schemes that use the available information to infer the location of the PU receivers, and account for channel state information (CSI) imperfections present in the overall network optimization procedure.

The present paper advocates the novel notion of *receiver map* as a tool for unveiling areas where PU receivers are located, with the objective of limiting the interference inflicted to those locations. These maps are tracked using a recursive Bayesian estimator [15], which is based on a 1-bit message broadcasted by the PU system whenever the instantaneous interference inflicted to a PU receiver exceeds a given tolerable level. These simple interference announcements are reminiscent of modern real-time social messaging systems - thus, the term "interference tweets" - and puts the hierarchical spectrum access paradigm closer to a community-based wireless networking setup. Two broadcasting setups are considered. In the first one, a binary interference announcement is sent by e.g., a base station or a primary network controller (NC); in this message, no information regarding the PU(s) that was (were) interfered is provided. In the second case, the number of PUs interfered and their identities are known; this is because this information is specified in the tweet sent by the primary NC (requiring a few additional bits to indicate the interfered PUs), or, because the PU receivers sent the tweet themselves (and the PU identifier is included as usual in the packet header). The case where the interference tweet is not correctly received by the SU system due to e.g., deep fading, is also analyzed. Bayesian localization using quantized RSS measurements was considered in e.g., [16], [17]. Instead of RSS samples, areas where PU receivers are likely to reside are unveiled here by exploiting the PU interference tweets and the distribution of SU-to-PU propagation gains.

In the mainstream CR literature, SUs are de facto envisioned to gain access to licensed frequencies without requiring any modification to communication and operational protocols of primary systems. Requiring the PU system to broadcast one bit when disruptive interference occurs, involves a slight modification of the primary system operation. However, it will be shown that significant improvements in spectrum (re)use efficiency can be obtained with this minimal system interplay, thus reaping off the benefits offered by the CR technology to the full extent. In setups where the broadcasting of tweets is not feasible, the secondary network can still estimate the receiver map by e.g., overhearing retransmission requests of the PUs [5], [18]. The schemes designed in this paper can be naturally extended to account for this sensing mode, thanks to their ability to handle uncertain/erroneous interference notifications; however, map estimation accuracy and overall performance of the secondary network certainly deteriorate

relative to the case where tweets are broadcasted.

Similar to [9], [19], the proposed cross-layer resource allocation (RA) scheme is designed as the solution of a constrained optimization problem featuring long-term probability-of-interference constraints. Specific to the present formulation is the the presence of uncertain SU-to-PU propagation gains *and* uncertain locations of PUs, as well as a multi-hop secondary network setup. Access among SUs is assumed orthogonal, and the resources at the transport, network, link and physical layers are adapted to the *time-varying* SU-to-SU *channels and* the receiver *maps*. Although nonconvex, the formulated problem has zero duality gap, and it is optimally solved using a Lagrangian dual approach. Taking advantage of the problem separability across SUs in the dual domain, computationally-affordable optimal solvers for transmit-powers, scheduling and routing variables, as well as exogenous traffic rates are developed.

The rest of the paper is organized as follows. System model and problem formulation are presented in Section II. The RA is solved optimally in Section III. Section IV presents the receiver map machinery. Numerical experiments are provided in Section V, and Section VI concludes the paper.[1]

II. Modeling and Problem formulation

A. Primary and secondary state information

Consider a multi-hop SU network comprising M nodes $\{U_m\}_{m=1}^M$ deployed over an area $\mathcal{A} \subset \mathbb{R}^2$. Assume that SUs share a flat-fading frequency band with an incumbent PU system in an underlay setup [1]; though, methods and results presented throughout the paper can be readily extended to multiple (frequency-selective) bands. Based on the output of the spectrum sensing stage [11]–[13], SUs implement adaptive RA to maximize network performance, while protecting the PU system from excessive interference.

[1]*Notation:* $\mathbb{E}_{\mathbf{g}}[\cdot]$ denotes expectation with respect to (w.r.t.) the random process $\mathbf{g}$; $\Pr\{A\}$ the probability of event A; x^* the optimal value of x; $\mathbb{1}_{\{\cdot\}}$ the indicator function ($\mathbb{1}_{\{x\}} = 1$ if x is true, and zero otherwise); $[x]_+$ the projection of the scalar x onto the non-negative outhunt; and, $[x]_a^b := \min\{\max\{x, a\}, b\}$ the projection of the scalar x onto $[a, b]$. Given a function $V(x)$, $\dot{V}(x)$ denotes the derivative function or the derivative of $V(x)$, and $(V)^{-1}(x)$ the inverse function, provided it exists. Finally, $\wedge$ denotes the "and" logical operator.

When spectral resources are shared in a hierarchical setup, the channel state information (CSI) available to the SU network is heterogeneous; in fact, the accuracy of the CSI for a given link typically depends on whether PUs or SUs are involved [2]. Provided the spectrum is available for the SUs to transmit, the SU-to-SU channels can be readily acquired by employing conventional training-based channel estimators. For this reason, the state of the SU-to-SU channels is considered known. The instantaneous gain of link $U_m \rightarrow U_n$ is denoted as $g_{m,n}$, and it is given by the squared magnitude of the small-scale fading realization scaled by the average signal-to-interference-plus-noise ratio (SINR) [20], so that it accounts also for the interference inflicted to SUs by the PU sources.

Suppose now that PU transmitters communicate with Q PU *receivers* geolocated at $\{\mathbf{x}^{(q)} \in \mathcal{A}\}_{q=1}^{Q}$, and denote by $h_{m,\mathbf{x}^{(q)}}$ the instantaneous channel gain between U_m and position $\mathbf{x}^{(q)}$. Since PUs have generally no incentive to use primary spectral resources to exchange synchronization and channel training signals with SUs [1], training-based channel estimation cannot be employed at the SU end to acquire $\{h_{m,\mathbf{x}^{(q)}}\}$. Thus, even though the *average link gain* can be obtained based on locations $\{\mathbf{x}^{(q)} \in \mathcal{A}\}_{q=1}^{Q}$ [20], the instantaneous value of the primary link is *uncertain* due to random fast fading effects. Consequently, SU m cannot assess precisely the interference that it will cause to PU q. Hereafter, it is assumed that only the joint distribution of processes $\{h_{m,\mathbf{x}^{(q)}}\}$ is known to the SU network, which is denoted as $\phi_h(\{h_{m,\mathbf{x}^{(q)}}\})$. Thus, given the maximum instantaneous interference power I tolerable by the PUs, the secondary network can determine the interference probabilities at each location $\mathbf{x}^{(q)}$. For instance, in an orthogonal access mode, if U_m is scheduled to access the channel with a transmit-power p, the probability of causing interference to PU receiver q is $\Pr\left\{p\, h_{m,\mathbf{x}^{(q)}} > I\right\}$.

Acquiring the location of passive PU receivers is challenging because conventional spectrum sensing schemes aim to detect and localize active PU *sources* [11]–[13]. PU receivers remain silent most of the time, and their signalling messages may not be easily detected (especially if they are sent over a dedicated control channel). As a consequence, locations $\{\mathbf{x}^{(q)} \in \mathcal{A}\}_{q=1}^{Q}$ are generally *uncertain*. Let $z_{\mathbf{x}}^{(q)}$ be a binary variable taking the value 1 if PU receiver q is located at $\mathbf{x} \in \mathcal{A}$. Further, consider discretizing the PU coverage region into a set of grid points $\mathcal{G} := \{\mathbf{x}_g\}$ representing *potential* locations for the PU receivers. In lieu of $\{z_{\mathbf{x}}^{(q)}\}$, the idea here is to use

the probabilities $\beta_{\mathbf{x}}^{(q)} := \Pr\{z_{\mathbf{x}}^{(q)} = 1\}$, $\forall\ \mathbf{x} \in \mathcal{G}$, to identify areas where a PU receiver q is more likely to reside, and limit the interference accordingly. To this end, the following is assumed.

(as1) $\{g_{m,n}\}$ and $\{h_{m,\mathbf{x}^{(q)}}\}$ are mutually independent; and,

(as2) $z_{\mathbf{x}}^{(q)}$ and $z_{\mathbf{x}}^{(v)}$, with $q \neq v$, are independent.

Assumption *(as2)* presupposes that each PU receiver has its own mobility pattern, while *(as1)* implies that the uncertainty of $\{h_{m,\mathbf{x}^{(q)}}\}$ is spatially uncorrelated. This is certainly the case when, e.g., spatial correlation of shadowing is negligible [5], [13], or path loss and shadowing are accurately acquired as in e.g., [21]. Next, sets $\mathbf{g} := \{g_{m,n}\}$ and $\mathbf{s} := \{\phi_h\} \cup \{\beta_{\mathbf{x}}^{(q)}\}$ collect the available secondary CSI, and the statistical primary state information (PSI), respectively.

B. RA under primary state uncertainty

Application-level data packets are generated exogenously at the SUs, and routed throughout the network to the intended destination(s). Packet streams are referred to as flows, and they are indexed by k. The destination of each flow is denoted by $d(k)$. Different traffic flows (e.g., video, voice, or elastic data) may be generated at the same SU, and routed towards the same destination. For each flow k, packet arrivals at U_m are modeled by a stationary stochastic process with mean $a_m^k \geq 0$.

Let $r_{m,n}^k(\mathbf{g}, \mathbf{s}) \geq 0$ be the instantaneous rate used for routing packets of flow k on link $U_m \rightarrow U_n$, during the state realizations $\mathbf{g}$ and $\mathbf{s}$. Suppose that SUs are equipped with queues (buffers) to store all incoming packets (exogenous and endogenous), so that no packets are discarded. Let $b_m^k[t]$ denote the amount of packets of flow k that at time t are stored in the queue of node m. In this paper, queues are deemed stable if $\lim_{t\rightarrow+\infty}(1/t)\sum_{\tau=1}^{t}\mathbb{E}[b_m^k[\tau]] < \infty$ [22]. Accordingly, for queues to be stable, exogenous and endogenous rates need to satisfy the following necessary condition for all m and k:

$$a_m^k + \sum_{n\in\mathcal{N}_m}\mathbb{E}_{\mathbf{g},\mathbf{s}}\left[r_{n,m}^k(\mathbf{g},\mathbf{s})\right] \leq \sum_{n\in\mathcal{N}_m}\mathbb{E}_{\mathbf{g},\mathbf{s}}\left[r_{m,n}^k(\mathbf{g},\mathbf{s})\right] \quad \forall\ m \neq d(k) \tag{1}$$

where $\mathcal{N}_m \subset \{1,\ldots,M\}$ denotes the set of one-hop neighboring nodes of U_m. SUs implement flow control, and thus the rates $\{a_m^k\}$ will be variables of the RA problem. Clearly,

$\{\mathbb{E}_{\mathbf{g},\mathbf{s}}[r^k_{m,n}]\}_{n\in\mathcal{N}_m}$ specify the average amount of packets that are routed through each of the U_m's outgoing links.

As for the medium access layer, define a binary scheduling variable $w_{m,n}$ taking the value 1 if U_m is scheduled to transmit to its neighbor U_n, and 0 otherwise. Secondary transmissions are assumed orthogonal. Orthogonal access is adopted by a gamut of wireless systems because of its low-complexity implementation. It also enables a (nearly) optimal network operation under moderate-to-strong interference transmission scenarios [23]. Assuming that one secondary link is scheduled per time slot, it follows that

$$\sum_{(m,n)\in\mathcal{E}} w_{m,n}(\mathbf{g},\mathbf{s}) \leq 1 \tag{2}$$

where $\mathcal{E} := \{(m,n) : n \in \mathcal{N}_m, m = 1,\ldots,M\}$ represents the set of SU-to-SU links. When $\sum_{(m,n)\in\mathcal{E}} w_{m,n}(\mathbf{g},\mathbf{s}) = 0$, no SU transmits because either the quality of all SU-to-SU channels is poor, or, excessive interference is inflicted to PUs.

At the physical layer, instantaneous rate and transmit power variables are coupled, and this rate-power coupling is modeled here using Shannon's capacity formula $C_{m,n}(g_{m,n},p_{m,n}) = W\log(1+ p_{m,n}g_{m,n}/\kappa_{m,n})$, where $\kappa_{m,n}$ represents the coding scheme-dependent SINR gap [20], and W is the bandwidth of the primary channel that is to be (re-)used. The premise for this capacity formula is that channels $\{g_{m,n}\}$ can be estimated perfectly. Notice however that errors in the estimation of $\{g_{m,n}\}$ can be readily accounted for as shown in, e.g., [24]. Let $\bar{p}_m$ denote the average transmit-power of U_m, which can be expressed as

$$\bar{p}_m = \mathbb{E}_{\mathbf{g},\mathbf{s}}\left[\sum_{n\in\mathcal{N}_m} w_{m,n}(\mathbf{g},\mathbf{s})p_{m,n}(\mathbf{g},\mathbf{s})\right]. \tag{3}$$

Power transmitted by the SUs have to obey two different constraints. First, due to spectrum mask specifications, the instantaneous power $p_{m,n}$ cannot exceed a pre-defined limit $p_m^{\max}$. Second, the average power satisfies $\bar{p}_m \leq \bar{p}_m^{\max}$.

To account for the interference inflicted to the PU system [1], define the binary variable $i^{(q)}(\{p_{m,n}\},\mathbf{s})$ as

$$i^{(q)}(\{p_{m,n}\},\mathbf{s}) := \sum_{\mathbf{x}\in\mathcal{G}} \mathbb{1}_{\{\sum_{(m,n)\in\mathcal{E}} w_{m,n}(\mathbf{g},\mathbf{s})p_{m,n}(\mathbf{g},\mathbf{s})h_{m,\mathbf{x}^{(q)}}>I\}}\tilde{z}^{(q)}_{\mathbf{x}}. \tag{4}$$

Since $z_{\mathbf{x}}^{(q)}$ pinpoints the location of PU receiver q, variable $i^{(q)}(\{p_{m,n}\},\mathbf{s})$ clearly indicates whether or not excessive instantaneous interference is inflicted to PU receiver q. Further, define the binary random variable

$$i(\{p_{m,n}\},\mathbf{s}) := 1-\prod_{q=1}^{Q}(1-i^{(q)}(\{p_{m,n}\},\mathbf{s}))\,, \tag{5}$$

which is 1 if one or more PU receivers are interfered. Since $w_{m,n}(\mathbf{g},\mathbf{s})\in\{0,1\}$, and at most one secondary link is active per time slot, $i(\{p_{m,n}(\mathbf{g},\mathbf{s})\},\mathbf{s})$ can be equivalently rewritten as

$$i(\{p_{m,n}(\mathbf{g},\mathbf{s})\},\mathbf{s}) = \sum_{(m,n)\in\mathcal{E}} w_{m,n}(\mathbf{g},\mathbf{s})i_{m,n}(p_{m,n}(\mathbf{g},\mathbf{s}),\mathbf{s}) \tag{6}$$

where

$$i_{m,n}(p,\mathbf{s}) := 1-\prod_{q=1}^{Q}\Big(1-\sum_{\mathbf{x}\in\mathcal{G}}\mathbb{1}_{\{ph_{m,\mathbf{x}^{(q)}}>I\}}z_{\mathbf{x}}^{(q)}\Big) \tag{7}$$

depends only on the transmit-power of SU m and the scheduling variable $w_{m,n}$. Let $i^{\max}\in(0,1)$ denote the maximum long-term probability (rate) of interference. Then, the following constraint must hold

$$\mathbb{E}_{\mathbf{g},\mathbf{s}}\left[\sum_{(m,n)\in\mathcal{E}} w_{m,n}(\mathbf{g},\mathbf{s})i_{m,n}(p_{m,n}(\mathbf{g},\mathbf{s}),\mathbf{s})\right]\leq i^{\max}\,. \tag{8}$$

SU-to-SU channels $\mathbf{g}$ vary across time due to fading. Thus, the SU network operates in a time-slotted setup, where the duration of each slot (indexed by t) corresponds to the coherence time of the small-scale fading process. The PSI $\mathbf{s}$ may also vary (due to, e.g., PU mobility), but at a larger time scale. Thus, since $\{r_{n,m}^k, w_{m,n}, p_{m,n}\}$ are computed based on $\mathbf{g},\mathbf{s}$, it follows that $\{r_{n,m}^k, w_{m,n}, p_{m,n}\}$ vary with time too. Henceforth, $\mathbf{g}$, $\mathbf{s}$, $r_{n,m}^k(\mathbf{g},\mathbf{s})$, $w_{m,n}(\mathbf{g},\mathbf{s})$, and $p_{m,n}(\mathbf{g},\mathbf{s})$ will be replaced by $\mathbf{g}[t]$, $\mathbf{s}[t]$, $r_{n,m}^k[t]$, $w_{m,n}[t]$, and $p_{m,n}[t]$ whenever time dependence is to be stressed. The metric to be optimized will be designed to discourage high average power consumptions, while promoting high exogenous traffic rates. To this end, let $V_m^k(a_m^k)$ denote a concave, non-decreasing, utility function quantifying the reward associated with the exogenous rate a_m^k, and $J_m(\bar{p}_m)$ be a convex, non-decreasing, function representing the cost incurred by U_m when its average transmit-power is $\bar{p}_m$ [19]. The metric to be maximized is then

$$f(\{a_m^k\},\{\bar{p}_m\}) := \sum_{m,k} V_m^k(a_m^k) - \sum_m J_m(\bar{p}_m)\,. \tag{9}$$

Based on the preceding discussion and with $\mathcal{Y} := \{a_m^k, \bar{p}_m, r_{n,m}^k(\mathbf{g},\mathbf{s}), w_{m,n}(\mathbf{g},\mathbf{s}), p_{m,n}(\mathbf{g},\mathbf{s}), \forall m,n \in \mathcal{N}_m, \mathbf{g}, \mathbf{s}\}$ collecting all the design variables, the optimal cross-layer RA for the SU network subject to ("s. to") interference constraints is designed as the solution of

$$\mathsf{P}^* := \max_{\mathcal{Y}} \sum_{m,k} V_m^k(a_m^k) - \sum_m J_m(\bar{p}_m) \tag{10a}$$

$$\text{s.to}: (1),\ (2),\ (8),\ \text{and} \tag{10b}$$

$$\sum_k r_{m,n}^k(\mathbf{g},\mathbf{s}) \leq w_{m,n}(\mathbf{g},\mathbf{s}) C_{m,n}(\mathbf{g}, p_{m,n}(\mathbf{g},\mathbf{s})) \tag{10c}$$

$$\mathbb{E}_{\mathbf{g},\mathbf{s}}\left[\sum_{n\in\mathcal{N}_m} w_{m,n}(\mathbf{g},\mathbf{s}) p_{m,n}(\mathbf{g},\mathbf{s})\right] \leq \bar{p}_m \tag{10d}$$

$$w_{m,n}(\mathbf{g},\mathbf{s}) \in \{0,1\},\ a_m^{k,\min} \leq a_m^k \leq a_m^{k,\max}\ \ 0 \leq r_{m,n}^k \tag{10e}$$

$$0 \leq p_{m,n} \leq p_m^{\max},\ \ 0 \leq \bar{p}_{m,n} \leq \bar{p}_m^{\max} \tag{10f}$$

where $a_m^{k,\min}$ and $a_m^{k,\max}$ are arrival rate requirements; (10d) has been relaxed and written as an inequality [cf. (3)] without loss of optimality; and (10c) dictates that the rate at the network level cannot exceed the one at the link layer. If needed, (10c) can be modified to account for losses due to packet/frame headers.

Unfortunately, (10) is a challenging non-convex problem. Specifically, nonconvexity emerges because:

i) $\{w_{m,n}(\mathbf{g},\mathbf{s})\}$ are binary variables;

ii) the monomials $w_{m,n}(\mathbf{g},\mathbf{s})p_{m,n}(\mathbf{g},\mathbf{s})$ and $w_{m,n}(\mathbf{g},\mathbf{s})C_{m,n}(p_{m,n}(\mathbf{g},\mathbf{s}))$ are not *jointly* convex in $w_{m,n}$ and $p_{m,n}$; and,

iii) the interference constraint (8) is nonconvex. Despite these difficulties, it will be shown in the ensuing section that the *optimal* solution can be obtained.

III. Optimal Adaptive RA

Consider first relaxing the binary scheduling constraints $w_{m,n}(\mathbf{g},\mathbf{s}) \in \{0,1\}$ as $w_{m,n}(\mathbf{g},\mathbf{s}) \in [0,1]$. Since constraints (2), (10c), (10d), and (8) are linear w.r.t. $w_{m,n}(\mathbf{g},\mathbf{s})$, each of the optimal arguments $\{w_{m,n}^*\}$ of the resultant relaxed problem lies at one of the boundaries of interval $[0,1]$; thus, $\{w_{m,n}^*\}$ in the relaxed problem coincide with the ones of (10). See the Appendix for a

formal discussion. Next, to cope with the nonconvexity of the monomial $w_{m,n}(\mathbf{g},\mathbf{s})p_{m,n}(\mathbf{g},\mathbf{s})$ and function $w_{m,n}(\mathbf{g},\mathbf{s})C_{m,n}(\mathbf{g},p_{m,n}(\mathbf{g},\mathbf{s}))$, consider introducing the auxiliary variables $\tilde{p}_{m,n}(\mathbf{g},\mathbf{s}) := w_{m,n}(\mathbf{g},\mathbf{s})p_{m,n}(\mathbf{g},\mathbf{s})$, $(m,n) \in \mathcal{E}$. It can be readily verified that the Hessian of the function $w_{m,n}(\mathbf{g},\mathbf{s})C_{m,n}(\mathbf{g},\tilde{p}_{m,n}(\mathbf{g},\mathbf{s})/w_{m,n}(\mathbf{g},\mathbf{s}))$ is seminegative definite, and thus the surrogate of (10c) is convex. Unfortunately, there is no immediate way to address the nonconvexity of (8). Nevertheless, one can leverage the results of [25, Thm. 1] to show that the duality gap is *zero*, and adopt a Lagrangian dual approach *without* loss of optimality. What is more, it will be shown that the minimization of the Lagrangian can be carried out in a computationally-efficient manner, thank to a favorable structure of the Lagrangian.

To this end, consider dualizing the average constraints, and let $\{\lambda_m^k\}$, θ, and $\{\pi_m\}$ denote the multipliers associated with (1), (8), and (10d), respectively. Thus, with $\mathbf{d} := \{\lambda_m^k, \pi_m, \theta\}$, the (partial) Lagrangian of (10) amounts to

$$\begin{aligned}\mathcal{L}(\mathcal{Y},\mathbf{d}) := &\sum_{m,k} V_m^k(a_m^k) - \sum_m J_m(\bar{p}_m) \\ &- \sum_{m,k} \lambda_m^k \left(a_m^k + \sum_{n\in\mathcal{N}_m} \left(\mathbb{E}_{\mathbf{g},\mathbf{s}} \left[r_{n,m}^k(\mathbf{g},\mathbf{s}) - r_{m,n}^k(\mathbf{g},\mathbf{s}) \right] \right) \right) \\ &- \theta \left(\mathbb{E}_{\mathbf{g},\mathbf{s}} \left[\sum_{(m,n)\in\mathcal{E}} w_{m,n}(\mathbf{g},\mathbf{s}) i_{m,n}(\tilde{p}_{m,n},\mathbf{s}) \right] - i^{\max} \right) \\ &- \sum_m \pi_m \left(\mathbb{E}_{\mathbf{g},\mathbf{s}} \left[\sum_{n\in\mathcal{N}_m} \tilde{p}_{m,n}(\mathbf{g},\mathbf{s}) \right] - \bar{p}_m \right). \end{aligned} \tag{11}$$

Assuming that the optimal multipliers $\{\lambda_m^{k*}, \pi_m^*, \theta^*\}$ are available, the optimal primal variables can be computed as follows.

Proposition 1. *The optimal average transmit-power $\bar{p}_m^*$ of node U_m is found as the solution of the scalar convex program*

$$\bar{p}_m^*(\pi_m^*) := \underset{0\le\bar{p}_m\le\bar{p}_m^{\max}}{\arg\max} \; - J_m(\bar{p}_m) + \pi_m^* \bar{p}_m \,. \tag{12}$$

If $\dot{J}_m(\pi_m)$ exists and is invertible, it follows that

$$\bar{p}_m(\pi_m^*) = \left[(\dot{J}_m)^{-1}(\pi_m^*) \right]_0^{\bar{p}_m^{\max}}. \tag{13}$$

This result can be obtained by isolating the terms in $\mathcal{L}(\mathcal{Y}, \mathbf{d}^*)$ that depend on $\{\bar{p}_m\}$, maximizing those terms separately, and subsequently projecting the solution onto the feasible set $[0, \bar{p}_m^{\max}]$. Following similar steps, the optimal average exogenous rates can be found as specified next.

Proposition 2. *Given the optimal dual variables $\{\lambda_m^{k*}\}$, the optimal exogenous rates $\{a_m^{k*}\}$ are*

$$a_m^{k*}(\lambda_m^{k*}) = \underset{a_m^{k,\min} \le a \le a_m^{k,\max}}{\arg\max} \; V_m^k(a) - \lambda_m^{k*} a \,. \tag{14}$$

When the inverse of $\dot{V}_m^k(a)$ exists, a_m^{k*} can be obtained in closed form as

$$a_m^{k*}(\lambda_m^{k*}) = \left[(\dot{V}_m^k)^{-1}(\lambda_m^{k*}) \right]_{a_m^{k,\min}}^{a_m^{k,\max}} . \tag{15}$$

As expected, the optimal flow policy (14) takes into account both the reward $V_m^k(a_m^k)$, and the "price" λ_m^{k*} for injecting exogenous traffic at a rate a_m^k into the network. Similarly, the optimal average power in (12) is set by balancing the cost $J_m(\bar{p}_m)$ with the reward represented by π_m^*.

Towards finding the optimal routing, scheduling, and instantaneous transmit-powers, define for each link (m, n) the coefficients

$$\lambda_{m,n}^{k*} := \lambda_m^{k*} - \lambda_n^{k*} \quad \text{and} \quad \lambda_{m,n}^* := \max_k \{\lambda_{m,n}^{k*}\} \tag{16}$$

along with the functional

$$\varphi_{m,n}(\mathbf{g}[t], p, \mathbf{d}^*) := \left[\lambda_{m,n}^* C_{m,n}(\mathbf{g}[t], p) - \pi_m^* p - \theta^* \mathbb{E}_{\mathbf{s}[t]} \left[i_{m,n}(p, \mathbf{s}[t]) \right] \right]_+ \tag{17}$$

where $\{\mathbf{g}[t], \mathbf{s}[t]\}$ are the realizations of $\{\mathbf{g}, \mathbf{s}\}$ at slot t. Under *(as1)–(as2)*, the expected value $\mathbb{E}_{\mathbf{s}[t]} \left[i_{m,n}(p, \mathbf{s}[t]) \right]$ can be written as

$$\mathbb{E}_{\mathbf{s}[t]} \left[i_{m,n}(p, \mathbf{s}[t]) \right] = 1 - \prod_{q=1}^{Q} \Big(1 - \sum_{\mathbf{x} \in \mathcal{G}} \iota_{m,\mathbf{x}^{(q)}}(p, \mathbf{s}[t]) \beta_{\mathbf{x}}^{(q)} \Big) \tag{18}$$

with $\iota_{m,\mathbf{x}^{(q)}}(p, \mathbf{s}[t]) := \Pr\left\{ p \, h_{m,\mathbf{x}^{(q)}} > I \right\}$. The previous probability can be either evaluated numerically or, for tractable fading distributions, computed in closed form. For example, if $h_{m,\mathbf{x}}$ is Rayleigh distributed, then $\iota_{m,\mathbf{x}}(p, \mathbf{s}[t]) = e^{-I/(p \gamma_{m,\mathbf{x}}[t])}$ with $\gamma_{m,\mathbf{x}}$ denoting the path loss between SU U_m and grid point $\mathbf{x}$ [20].

Using (16) and (17), optimal rates $\{r_{m,n}^{k*}[t]\}$, scheduling variables $\{w_{m,n}^*[t]\}$, and instantaneous transmit-powers $\{p_{m,n}^*[t]\}$ are found as specified next (the proofs are outlined in the Appendix).

Proposition 3. *Given* $\mathbf{g}[t]$ *and* $\mathbf{s}[t]$*, the optimal* $\{p^*_{m,n}[t], w^*_{m,n}[t]\}$ *are*

$$p^*_{m,n}[t] := \left[\arg\max_{p}\ \varphi_m(\mathbf{g}[t], p, \mathbf{d}^*))\right]_0^{p_m^{\max}} \tag{19}$$

$$w^*_{m,n}[t] := \mathbb{1}_{\{(m,n)=\arg\max_{(i,j)\in\mathcal{E}}\varphi_{m,n}(\mathbf{g}[t],p^*_{m,n}[t],\mathbf{d}^*)\}}. \tag{20}$$

Proposition 4. *Per link* $(m,n)\in\mathcal{E}$*, define the set* $\mathcal{K}_{m,n}[t] := \{k : k = \arg\max_j\{\lambda^{j*}_{m,n}\} \wedge \lambda^{k*}_{m,n} \geq 0\}$*. Then, the optimal* $\{r^{k*}_{m,n}[t]\}$ *satisfy the following two conditions:*

r1) if $k \notin \mathcal{K}_{m,n}[t]$*, then* $r^{k*}_{m,n}[t] = 0$*; and,*

r2) if $|\mathcal{K}_{m,n}[t]| \geq 1$*, if follows that* $\sum_{k\in\mathcal{K}_{m,n}[t]} r^{k*}_{m,n}[t] = w^*_{m,n}[t]\, C_{m,n}(\mathbf{g}[t], p^*_{m,n}[t])$.

Clearly, when $|\mathcal{K}_{m,n}[t]| = 1$*, one has the "winner-takes-all" solution*

$$r^{k*}_{m,n}[t] = \mathbb{1}_{\{k\in\mathcal{K}_{m,n}[t]\}} w^*_{m,n}[t]\, C_{m,n}(\mathbf{g}[t], p^*_{m,n}[t])\,. \tag{21}$$

Key to understanding the solution of Proposition 3 is the definition of $\varphi_{m,n}(\mathbf{g}[t], p, \mathbf{d}^*)$. Intuitively, (17) can be interpreted as an instantaneous link-quality indicator, which dictates a trade-off between the instantaneous transmit-rate, transmit-power and interference (with the multipliers $\lambda^*_{m,n}$, π^*_m and θ^* representing the prices of the corresponding resources). Interestingly, (19) reveals that $p^*_{m,n}[t]$ is found by maximizing $\varphi_{m,n}(\mathbf{g}[t], p, \mathbf{d}^*)$, which does not depend on information of links other than $U_m \to U_n$. In other words, the optimization problem in the dual domain is separable across SU links (and time). For many fading distributions, (19) turns out to be nonconvex. However, since only one scalar variable is involved, the optimal transmit-power $p^*_{m,n}[t]$ can be found efficiently. Proposition 4 describes the operation of the routing protocol and establishes that only flows with the highest value of $\lambda^{k*}_{m,n}$ can be routed. Clearly, the multiplier λ^{k*}_m can be viewed as a congestion indicator of flow k at node m, so that the optimum solution dictates that flows have to follow routes that maximize the difference $\lambda^{k*}_{m,n} = \lambda^{k*}_n - \lambda^{k*}_m$. This reveals that the solution reduces the network congestion (in fact, links to the well-known *back-pressure* routing algorithm can be established [19]). Further, it worth stressing that the value of the channel gain of a SU-to-SU link does not affect how different flows share that link, but only the number of packets routed through it; i.e., only $C_{m,n}(\mathbf{g}[t], p^*_{m,n}[t])$.

The next subsection deals with the estimation of the optimum Lagrange multipliers. But first, a remark is in order.

Remark 1 (Contention graph). In lieu of (2), the notion of "contention graph" is oftentimes advocated in conventional multi-hop wireless setups to possibly activate multiple wireless links simultaneously; see e.g., [26], [27]. Taking a similar approach for the problem at hand is challenging because: *i)* presence of the probability-of-interference constraints would render the definition of such a graph non-trivial; and, *ii)* the power optimization would be coupled across SUs. Development of *approximate* solutions tailored to the problem at hand are left as future work.

A. Estimating the optimum Lagrange multipliers

Finding the optimal dual variables $\{\lambda_m^{k*}, \pi_m^*, \theta^*\}$ may be computational challenging because: *a)* classical iterative subgradient methods require, at each iteration, averaging over all $\mathbf{g}$ and $\mathbf{s}$ realizations; and, *b)* if either the channel statistics or the number of users change, $\{\lambda_m^{k*}, \pi_m^*, \theta^*\}$ must be re-computed. An effective alternative consists in resorting to stochastic approximation iterations [28], [29], whose goal is to obtain samples $\{\lambda_m^k[t], \pi_m[t], \theta[t]\}$, $t = 1, 2, \ldots$ that are nevertheless sufficiently close to the optimal dual variables.

The merit of stochastic approximation techniques is twofold: *i)* computational complexity of the stochastic approximation schemes is markedly lower than that of their off-line counterparts; and, *ii)* stochastic schemes can cope with non-stationary propagation channels and dynamic PU activities. With $\mu_\lambda > 0$, $\mu_\pi > 0$, and $\mu_\theta > 0$ denoting constant stepsizes, the following stochastic iterations yield the desired multipliers $\forall\, t$:

$$\lambda_m^k[t+1] = \Big[\lambda_m^k[t] + \mu_\lambda\Big(a_m^{k*}(\lambda_m^k[t]) + \sum_{n\in\mathcal{N}_m}(r_{n,m}^{k*}[t] - r_{m,n}^{k*})[t]\Big)\Big]_+ \tag{22}$$

$$\pi_m[t+1] = \Big[\pi_m[t] - \mu_\pi\Big(\bar{p}_m^*(\pi_m[t]) - \sum_{n\in\mathcal{N}_m} w_{m,n}^*[t]p_{m,n}^*[t]\Big)\Big]_+ \tag{23}$$

$$\theta[t+1] = \Big[\theta[t] - \mu_\theta\Big(i^{\max} - i(\{p_{m,n}^*[t]\}, \mathbf{s}[t])\Big)\Big]_+ . \tag{24}$$

The update terms in the right hand side of (22)-(24) form an *unbiased* stochastic subgradient of the dual function of (10), and they are *bounded*; see, e.g., [30]. Using these two features, the following convergence and feasibility result can be established.

Proposition 5. *Define* $\mu := \max\{\mu_\lambda, \mu_\pi, \mu_\theta\}$; $\bar{P}[t] := \frac{1}{t}\sum_{\tau=1}^{t}\sum_m J_m(p_m^*[\tau]) - \sum_{m,k} V_m^k(a_m^{k*}(\lambda_m^k[\tau]))$; *and,* $\bar{i}[t] := \frac{1}{t}\sum_{\tau=1}^{t} i(\{p_{m,n}[\tau]\}, \mathbf{s}[\tau])$. *Then, it holds with probability one that as* $t \to \infty$ *the sample average of the stochastic RA:*

i) *is feasible and, thus,* $\bar{i}[t] \leq i^{max}$*; and,*

ii) *incurs minimal performance loss w.r.t. the optimal solution of* (10)*; i.e,* $\bar{P}[t] \geq P^* - \delta(\mu)$*, where* $\delta(\mu) \to 0$ *as* $\mu \to 0$.

A proof of this result is not presented here due to space limitations, but it relies on the convergence of stochastic (epsilon) subgradient methods and can be obtained following the lines of [19], [29]. The key to prove *i)* is to show that the stochastic multipliers are bounded. This can be readily used to show the asymptotic feasibility of the sample averages of the stochastic subgradients, i.e., of the update terms in (22)-(24). The proof for *ii)* is a bit more intricate and leverages properties of the dual function, the convexity of the objective function in (10a), and the bounds on the stochastic updates. It turns out that the loss of optimality $\delta(\mu)$ is linear w.r.t. both μ and G, which represents an upperbound on the expected squared norm of the stochastic subgradient. Clearly, this implies that $\delta(\mu) \to 0$ as $\mu \to 0$.

B. Individual interference constraints

The developed RA scheme controls the interference inflicted to the primary *system*. However, it may turn that some PUs are interfered more frequently than others. To eliminate this discrepancy, probability-of-interference constraints can be placed on a per-PU receiver basis. The changes required in the optimal RA schemes to address this case are oulined next.

Define as $i_{m,n}^{(q)}(p, \mathbf{s}) := \sum_{\mathbf{x}\in\mathcal{G}} z_{\mathbf{x}}^{(q)} \mathbb{1}_{\{ph_{m,\mathbf{x}^{(q)}} > I\}}$ [cf. (7)] the probability of interfering with the PU receiver q when link $U_m \to U_n$ is scheduled. Then, the individual probability-of-interference constraints amount to [cf. (8)]

$$\mathbb{E}_{\mathbf{g},\mathbf{s}}\left[\sum_{(m,n)\in\mathcal{E}} w_{m,n}(\mathbf{g},\mathbf{s}) i_{m,n}^{(q)}(p_{m,n}(\mathbf{g},\mathbf{s}),\mathbf{s})\right] \leq i^{q,\max} \tag{25}$$

where $i^{q,\max}$ can either be set to the same value for all q, or, be customized. The next step is to modify the optimization problem (10) by replacing the single constraint (8) with the Q constraints (one per user) in (25). Each of the new constraints is dualized (with θ^q denoting

the corresponding multiplier) and incorporated into the Lagrangian in (11). The only change required in the expressions for the optimal RA is re-definition of the link-quality indicator in (17) as $\varphi_{m,n}(\mathbf{g}[t],p,\mathbf{d}^*) := [\lambda^*_{m,n}C_{m,n}(\mathbf{g}[t],p) - \pi^*_m p - \sum_q \theta^{q*}\mathbb{E}_{\mathbf{s}[t]}[i^{(q)}_{m,n}(p,\mathbf{s}[t])]]_+$. All other expressions for the optimal RA (including results in Propositions 1-4) remain the same.

The last step is to modify the stochastic update for the multiplier in (24). Instead of the single update for $\theta[t+1]$, the following Q updates are needed $\theta^q[t+1] = [\theta^q[t] - \mu_\theta(i^{\max}_{(q)} - i^{(q)}[t])]_+$, where $i^{(q)}[t] = 1$ if the PU receiver q has been interfered. Such an information is either broadcasted by the PU system or estimated from the available observations (see next section for details). If all constraints are active, then all the multipliers will be non-zero. However, there are scenarios where that would not be the case, e.g., if a PU receiver is very far away. In those cases, the stochastic estimate of the corresponding multiplier remains zero most of the time.

IV. Receiver-map estimation

The SU network relies on perfect CSI $\mathbf{g}$, probabilities $\{\iota_{m,n,\mathbf{x}}\}$ and the PU receivers' spatial distribution $\{\beta^{(q)}_{\mathbf{x}}\}$ to schedule SU transmissions, while adhering to the long-term interference constraints [cf. (17)]. The SU-to-SU gains $\mathbf{g}$ are acquired via conventional sensing. Moreover, once the virtual grid $\mathcal{G}$ is chosen, $\{\iota_{m,n,\mathbf{x}}\}$ can be computed as a function of the transmit-powers $\{p_{m,n}\}$. The aim here is to develop an online Bayesian estimator for $\{\beta^{(q)}_{\mathbf{x}}\}$, based on a minimal interplay between PU and SU systems. Specifically, the following setup is considered.

(as3) The PU system notifies the secondary network if disruptive interference occurrs to one or more PU receivers.

Two interference announcement strategies are considered:

(c1) the PU system broadcasts the message $i^{(q)}[t] = 1$ to notify that the event $p^*_{m^*,n^*}h_{m^*,\mathbf{x}^{(q)}} > I$ occurred; and,

(c2) the generic message $i[t] = 1$ is transmitted if at least one of the PU receivers were disruptively interfered.

In both setups, just *one*-bit is sufficient to notify the SU system that the instantaneous interference inflicted to one or more PU receivers exceeds the tolerable level I. In *(c2)*, this interference tweet is sent by, e.g., a base station or a primary NC. In this message, no information regarding the

PU user(s) interfered is provided. As for *(c1)*, the interference tweet can be sent by either the primary NC (requiring additional few bits to indicate the PU interfered), or, by the interfered PU receivers themselves (with the PU identifier included as usual in the packet header).

Similar modeling assumptions were made in, e.g., [5] and [18] (see also references therein), where the PU's Automatic Repeat-reQuests (ARQs) are assumed to be either exchanged or eavesdropped by the SU transceivers. With the overheard ARQs, the SUs can evaluate the outage rates of ongoing PU communications, and adjust their transmit-powers accordingly [5]. In lieu of outage rates, PU receiver locations may be estimated. However, localization based on RSS measurements over a single ARQ packet is challenging because of, e.g., PU mobility and fast time-varying fading. A more conservative (but suboptimal) approach that bypasses the need to know PU receiver locations is to guarantee that the interference does not exceed a prescribed level at any boundary point of the PU transmitters' coverage region [10], [13], [14], which can be estimated during the sensing phase [11], [13]. This amounts to arranging $Q = |\mathcal{G}|$ grid points in the boundary of the coverage region, and setting $\beta_{\mathbf{x}}^{(q)} = 1$ for all $q = 1, \ldots, Q$.

A. Per-PU receiver notification

To account for PU mobility, we assume that:

(as4) $z_{\mathbf{x}}^{(p)}[t]$ is a first-order (spatiotemporal) Markov process with *known* transition probabilities $\phi_{\mathbf{x},\mathbf{x}'}^{(q)}[t] := \Pr\{z_{\mathbf{x}}^{f,(q)}[t] = 1 | z_{\mathbf{x}'}^{(q)}[t-1] = 1\}$.

To decrease the computational burden, $\phi_{\mathbf{x},\mathbf{x}'}^{(q)}[t]$ are further assumed to be nonzero only if $\mathbf{x}' \in \mathcal{G}_{\mathbf{x}}$, where the set $\mathcal{G}_{\mathbf{x}}$ contains $\mathbf{x}$ and its neighboring grid points. Collect in the set $\mathcal{I}_t^{(q)} := \{i^{(q)}[\tau]\}_{\tau=1}^t$ the interference notifications up to time slot t, and define further the sets $\tilde{\mathcal{H}}_t^{(q)} := \mathcal{I}_{t-1}^{(q)} \cup \{p_{m,n}^*[t], w_{m,n}^*[t],\ \forall (m,n)\}_{\tau=1}^t$ and $\mathcal{H}_t^{(q)} := \tilde{\mathcal{H}}_t^{(q)} \cup i^{(q)}[t]$. Since the elements of $\mathcal{I}_t^{(q)}$ constitute the observed states of a Hidden Markov Model (HMM), a recursive Bayesian estimator can be implemented to acquire (and track) the posterior probability mass function of $\{z_{\mathbf{x}}^{(q)}\}_{\mathbf{x}\in\mathcal{G}}$. To this end, let $\hat{\beta}_{\mathbf{x}}^{(q)}[t|t-1] := \Pr\{z_{\mathbf{x}}^{(q)}[t] = 1 | \mathcal{H}_{t-1}^{(q)}\}$ and $\hat{\beta}_{\mathbf{x}}^{(q)}[t|t] := \Pr\{z_{\mathbf{x}}^{(q)}[t] = 1 | \mathcal{H}_t^{(q)}\}$ denote the instantaneous beliefs given $\mathcal{H}_{t-1}^{(q)}$ and $\mathcal{H}_t^{(q)}$, respectively. Finally, let $(m^*, n^*) := \arg\max_{(i,j)\in\mathcal{E}} w_{m,n}^*[t]$ denote the scheduled link at time t. Thus, the receiver maps can be recursively updated by performing the following steps per grid point $\mathbf{x}$ and PU receiver q (see,

e.g., [15]).

Prediction step:

$$\hat{\beta}^{(q)}_{\mathbf{x}}[t|t-1] = \sum_{\mathbf{x}' \in \mathcal{G}_{\mathbf{x}}} \phi^{(q)}_{\mathbf{x},\mathbf{x}'}[t] \hat{\beta}^{(q)}_{\mathbf{x}}[t-1|t-1]\,. \tag{26}$$

Correction step:

$$\hat{\beta}^{(q)}_{\mathbf{x}}[t|t] = \frac{\Pr\{i^{(q)}[t] = o | z^{(q)}_{\mathbf{x}}[t] = 1, \tilde{\mathcal{H}}^{(q)}_t\} \hat{\beta}^{(q)}_{\mathbf{x}}[t|t-1]}{\Pr\{i^{(q)}[t] = o | \tilde{\mathcal{H}}^{(q)}_t\}} \tag{27}$$

where $o \in \{0, 1\}$ denotes the value observed for $i^{(q)}[t]$.

Suppose that $i^{(q)}[t] = 1$. Then, noticing that $z^{(q)}_{\mathbf{x}}[t] = 1$ implies that $z^{(q)}_{\mathbf{x}'}[t] = 0$ for the grid points $\mathbf{x}' \in \mathcal{G} \backslash \{\mathbf{x}\}$, it follows that $\Pr\{i^{(q)}[t] = 1 | z^{(q)}_{\mathbf{x}}[t] = 1, \tilde{\mathcal{H}}^{(q)}_t\} = \iota_{m,\mathbf{x}}(p^*_{m^*,n^*}, \mathbf{s}[t])$. As for the denominator in (27), one only has to average the numerator over all possible locations. For $i^{(q)}[t] = 1$ this entails

$$\Pr\{i^{(q)}[t] = 1 | \tilde{\mathcal{H}}^{(q)}_t\} = \sum_{\mathbf{x}' \in \mathcal{G}} \Pr\left\{ i^{(q)}[t] = 1 | z^{(q)}_{\mathbf{x}'}[t] = 1, \tilde{\mathcal{H}}^{(q)}_t \right\} \hat{\beta}^{(q)}_{\mathbf{x}'}[t|t-1] \tag{28a}$$

$$= \sum_{\mathbf{x}' \in \mathcal{G}} \iota_{m,\mathbf{x}'}(p^*_{m^*,n^*}, \mathbf{s}[t]) \hat{\beta}^{(q)}_{\mathbf{x}'}[t|t-1]. \tag{28b}$$

Thus, when interference is inflicted to the PU receiver q, (27) can be simplified to:

$$\hat{\beta}^{(q)}_{\mathbf{x}}[t|t] = \frac{\iota_{m,\mathbf{x}}(p^*_{m^*,n^*}, \mathbf{s}[t]) \hat{\beta}^{(q)}_{\mathbf{x}}[t|t-1]}{\sum_{\mathbf{x}' \in \mathcal{G}_{\mathbf{x}}} \iota_{m,\mathbf{x}'}(p^*_{m^*,n^*}, \mathbf{s}[t])\, \hat{\beta}^{(q)}_{\mathbf{x}'}[t|t-1]} \tag{29}$$

and can be readily computed once the SU-to-grid point channel distribution is known. The counterpart of (37) for $i^{(q)}[t] = 0$ is computed in the obvious way.

In this setup, the secondary system *does not* require prior knowledge of Q. Rather, the set $\mathcal{Q}$ of PU receivers that can be potentially interfered is updated on-line based on the messages $\{i^{(q)}[\tau] = 1\}$. For example, $\mathcal{Q}[t] = \mathcal{Q}[t-1] \cup \{q\}$ whenever $i^{(q)}[t] = 1$ and $q \neq \mathcal{Q}[t-1]$. On the other hand, $\mathcal{Q}[t]$ is updated as $\mathcal{Q}[t] = \mathcal{Q}[t-1] \backslash \{q\}$ when no messages are received from PU q for a prolonged period of time.

B. System-wide interference announcement

Similar to Section IV-A, let $\mathcal{I}_t := \{i[\tau]\}_{\tau=1}^t$ denote the set collecting the interference notifications, and let $\tilde{\mathcal{H}}_t := \mathcal{I}_{t-1} \cup \{p^*_{m,n}[\tau], w^*_{m,n}[\tau],\ \forall (m,n)\}_{\tau=1}^t$ and $\mathcal{H}_t := \tilde{\mathcal{H}}_t \cup i[t]$. Further, re-define

the instantaneous beliefs $\hat{\beta}_{\mathbf{x}}^{(q)}[t|t-1]$ and $\hat{\beta}_{\mathbf{x}}^{(q)}[t|t-1]$ as $\beta_{\mathbf{x}}^{(q)}[t|t-1] := \Pr\{z_{\mathbf{x}}^{(q)}[t]=1|\mathcal{H}_{t-1}\}$ and $\beta_{\mathbf{x}}^{(q)}[t|t] := \Pr\{z_{\mathbf{x}}^{(q)}[t]=1|\mathcal{H}_{t}\}$, respectively. With $\mathcal{I}_t$ representing again the observed states of an HMM, the prediction step of the resultant recursive Bayesian estimator is computed as in (26). On the other hand, the correction step becomes in this case

$$\hat{\beta}_{\mathbf{x}}^{(q)}[t|t] = \frac{\Pr\{i[t]=o|z_{\mathbf{x}}^{(q)}[t]=1,\tilde{\mathcal{H}}_t\}\hat{\beta}_{\mathbf{x}}^{(q)}[t|t-1]}{\Pr\{i[t]=o|\tilde{\mathcal{H}}_t\}} \tag{30}$$

where $o \in \{0,1\}$ denotes the value observed for $i[t]$.

To further elaborate on (30), the following modeling assumption is made.

(as5) The value (or an upper bound) of Q is known.

Section V will illustrate that *(as5)* is not very restrictive, since just an upperbound on the number of PU receivers Q suffices to carry out the localization task. More sophisticated schemes that jointly estimate and track Q and $\{\beta_{\mathbf{x}}^{(q)}\}$ are of interest, but they will be the subject of future research. When $i[t]=0$, the denominator of (30) is given by

$$\Pr\{i[t]=0|\tilde{\mathcal{H}}_t\} = \Pr\{i^{(1)}[t]=0,\ldots,i^{(Q)}[t]=0|\tilde{\mathcal{H}}_t\} \tag{31a}$$

$$= \prod_{q=1}^{Q}\left(1-\Pr\{i^{(q)}[t]=1|\tilde{\mathcal{H}}_t\}\right) \tag{31b}$$

$$= \prod_{q=1}^{Q}\Big(1-\sum_{\mathbf{x}\in\mathcal{G}}\iota_{m,\mathbf{x}}(p^*_{m^*,n^*}[t],\mathbf{s}[t])\hat{\beta}_{\mathbf{x}}^{(q)}[t|t-1]\Big) \tag{31c}$$

where (31b) follows (31a) because of *(as1)* and *(as2)*. The latter assumption holds also when two (or more) PU receivers reside in proximity of the same grid point, provided they are a few wavelengths apart [20, Ch. 3]. Clearly, for $i[t]=1$, $\Pr\{i[t]=1|\tilde{\mathcal{H}}_t\}$ is readily obtained as $\Pr\{i[t]=1|\tilde{\mathcal{H}}_t\} = 1-\Pr\{i[t]=0|\tilde{\mathcal{H}}_t\}$. Using similar steps, one can show that $\Pr\{i[t]=0|z_{\mathbf{x}}^{(q)}[t]=1,\tilde{\mathcal{H}}_t\}$ can be re-expressed as

$$\Pr\{i[t]=0|z_{\mathbf{x}}^{(q)}[t]=1,\tilde{\mathcal{H}}_t\} = \Pr\{i^{(1)}[t]=0,\ldots,i^{(Q)}[t]=0|z_{\mathbf{x}}^{(q)}[t]=1,\tilde{\mathcal{H}}_t\} \tag{32a}$$

$$= \Pr\{i^{(q)}[t]=0|z_{\mathbf{x}}^{(q)}[t]=1,\tilde{\mathcal{H}}_t\} \times \prod_{u=1,u\neq q}^{Q}\left(1-\sum_{\mathbf{x}'\in\mathcal{G}}\iota_{m,\mathbf{x}'}(p^*_{m^*,n^*}[t],\mathbf{s}[t])\hat{\beta}_{\mathbf{x}'}^{(u)}[t|t-1]\right) \tag{32b}$$

where $\Pr\{i^{(q)}[t]=0|z_{\mathbf{x}}^{(q)}[t]=1,\tilde{\mathcal{H}}_t\}$ can be further expressed as $\Pr\{i^{(q)}[t]=0|z_{\mathbf{x}}^{(q)}[t]=1,\tilde{\mathcal{H}}_t\} = 1-\iota_{m,\mathbf{x}}(p^*_{m^*,n^*},\mathbf{s}[t])$.

C. Receiver-map-cognizant RA

The receiver maps are used to evaluate the interference term in functional $\varphi_{m,n}$ [cf. (18)], which clearly affects the computation of the optimal transmit-powers $p^*_{m,n}[t]$ and scheduling variables $w^*_{m,n}[t]$ [cf. (19)-(20)]. Equation (18) implies that if the location of the PU receivers is perfectly known, only their corresponding terms $\{\mathbf{x}^{(q)}\}_{q=1}^{Q}$ will enter in the summation. On the other hand, if the actual location is uncertain, the interference generated at each point of the grid will be weighted by the probability of the PU receiver residing there. Hence, at slot t, the beliefs $\{\hat{\beta}^{(q)}_{\mathbf{x}}[t|t-1]\}$ are used to obtain $\mathbb{E}_{\mathbf{s}[t]}\left[i_{m,n}(p,\mathbf{s}[t])\right]$ in (18).

The receiver maps can also be used to update the stochastic Lagrange multiplier associated with the interference constraint; i.e., $\theta[t]$ in (24). A simple way to update $\theta[t]$, which does not require use of the receiver maps, is to leverage the actual interference notification $i[t]$. In case of system-wide tweets, this amounts to setting $\theta[t+1]=[\theta[t]-\mu_\theta(i^{max}-i[t])]_+$. If such a notification contains errors, $i[t]$ has to be replaced by an unbiased estimate of the actual interference. A more elaborate alternative is to use the receiver maps to *estimate* the actual interference and then update the multiplier as $\theta[t+1]=[\theta[t]-\mu_\theta(i^{max}-\Pr\{i[t]=1|\mathcal{H}_t\})]_+$. In this case, the interference notification $i[t]$ is first employed to update the maps $\hat{\beta}^{(q)}_{\mathbf{x}}[t|t-1]$. Then, the updated maps $\hat{\beta}^{(q)}_{\mathbf{x}}[t|t]$ for all q and $\mathbf{x}$, and the RA at time t, are used to find $\Pr\{i[t]=1|\mathcal{H}_t\}$.

The proposed joint RA and receiver map estimation algorithm is tabulated as Algorithm 1.

D. Accounting for PU-SU communication errors

To account for errors in the messages notifying interference, miss-detection and false-alarm events are considered. In particular, let $P^{(q)}_{MD}$ denote the probability of missing an interference tweet sent by PU receiver q, and P_{MD} its counterpart in the setup *(c2)*. Further, let $P^{(q)}_{FA}$ and P_{FA} denote the probability that the messages $i^{(q)}[t]=1$ and $i[t]=1$, respectively, were received, but no actual interference was caused. In the following, such probabilities are assumed known.

While the expression for the prediction step in (26) remains the same, the correction step must be adjusted to account for decoding failures and false-interference notifications. The error-aware correction step is first developed for *(c1)*, and subsequently tailored for *(c2)*.

Algorithm 1 Joint RA and receiver-map estimation

Initialize $\mathcal{Y}[0]$, $\mathbf{d}[0]$, and $\{\hat{\beta}_{\mathbf{x}}^{(q)}[0|0]\}$.

for $t = 1, \ldots$ (repeat until convergence) **do**

[s1] Perform the prediction step (26).

[s2] Acquire SU-to-SU channels $\{g_{m,n}[t]\}$.

[s3] Obtain $\{a_m^{k*}(\mathbf{d}[t-1])\}, \{r_{m,n}^{k*}[t-1]\}, \{\bar{p}_m^*(\mathbf{d}[t-1])\}$ via (15), (21), and (12)

[s4] Obtain $\{w_{m,n}^*[t], p_{m,n}^*[t]\}$ via (19)–(20), where $\{\beta_{\mathbf{x}}^{(q)}\}$ in (18) is replaced by $\{\hat{\beta}_{\mathbf{x}}^{(q)}[t|t-1]\}$.

[s5] Update $\{\lambda_m^k[t]\}, \{\pi_m[t]\}$ via (22)–(23).

[s5] Receive $i^{(q)}[t]$ (or $i[t]$), if interference occurred.

[s6] Update $\theta[t]$ via (24), using the observed $i^{(q)}[t]$ (or $i[t]$).

[s7] Run the correction step (27) (or (30)).

end for

1) Per-PU notification: The main idea is to update the expressions for the variables involved in the correction step in (27) for both $i^{(q)}[t] = 1$ and $i^{(q)}[t] = 0$. Key to this end is to re-write the numerator of (27). Let first define the probabilities

$$P_{\mathbf{x},0}^{(q)}[t] := 1 - \iota_{m,\mathbf{x}}(p_{m^*,n^*}^*, \mathbf{s}[t]) \tag{33}$$

$$P_{\mathbf{x},1}^{(q)}[t] := \iota_{m,\mathbf{x}}(p_{m^*,n^*}^*, \mathbf{s}[t])\,. \tag{34}$$

Clearly, $P_{\mathbf{x},0}^{(q)}[t]$ is the probability of not inflicting interference at time t given the system history $\tilde{\mathcal{H}}_t$, and assuming that $z_{\mathbf{x}}^{(q)}[t] = 1$. Such probabilities are used to define the correction coefficients

$$c_{\mathbf{x}|0}^{(q)} := (1 - P_{FA}^{(q)})P_{\mathbf{x},0}^{(q)}[t] + P_{MD}^{(q)}P_{\mathbf{x},1}^{(q)}[t] \tag{35}$$

$$c_{\mathbf{x}|1}^{(q)} := P_{FA}^{(q)}P_{\mathbf{x},0}^{(q)}[t] + (1 - P_{MD}^{(q)})P_{\mathbf{x},1}^{(q)}[t], \tag{36}$$

which represent the probability of observing $i^q[t] = 0$ and $i^q[t] = 1$, respectively. With these definitions, the correction step for $i^q[t] = o$ is [cf. (27)]

$$\hat{\beta}_{\mathbf{x}}^{(q)}[t|t] = \frac{c_{\mathbf{x}|o}^{(q)}\hat{\beta}_{\mathbf{x}}^{(q)}[t|t-1]}{\sum_{\mathbf{x}'\in\mathcal{G}_{\mathbf{x}}} c_{\mathbf{x}'|o}^{(q)}\hat{\beta}_{\mathbf{x}'}^{(q)}[t|t-1]}\,. \tag{37}$$

Although $P_{MD}^{(q)}$ and $P_{FA}^{(q)}$ have been assumed constant across space, they can be rendered dependent on $\mathbf{x}$. For example, if the Bayesian estimator is implemented at a secondary NC, then

the miss-detection probability can be written as $P_{MD}^{(q)} = \Pr\{p^{(q)} h_{\mathbf{x},NC}/\sigma^2 \leq \Gamma\}$, where $h_{\mathbf{x},NC}$ is the PU-to-NC channel, $p^{(q)}$ the power transmitted by PU q, σ^2 the detector noise, and Γ the SINR threshold under which packet decoding is deemed unsuccessful. Clearly, this probability depends on $\mathbf{x}$ and should be written as $P_{MD,\mathbf{x}}^{(q)}$. Accounting for this dependence only requires replacing $P_{MD}^{(q)}$ and $P_{FA}^{(q)}$ with $P_{MD,\mathbf{x}}^{(q)}$ and $P_{FA,\mathbf{x}}^{(q)}$ in (35)-(36).

2) System-wide notification: The main difference compared to the previous case is that the expressions for $P_{\mathbf{x},0}^{(q)}[t]$ and $P_{\mathbf{x},1}^{(q)}[t]$, which account for the probabilities of (not) interfering the PU system at time t given the history $\tilde{\mathcal{H}}_t$ and $z_{\mathbf{x}}^{(q)}[t] = 1$, are more intricate. Specifically, instead of (33) and (34) we have

$$P_{\mathbf{x},0}^{(q)}[t] := \left(1 - \iota_{m,\mathbf{x}}(p^*_{m^*,n^*}, \mathbf{s}[t])\right) \times \prod_{u=1, u\neq q}^{Q} \left(1 - \sum_{\mathbf{x}' \in \mathcal{G}} \iota_{m,\mathbf{x}'}(p^*_{m^*,n^*}[t], \mathbf{s}[t]) \hat{\beta}_{\mathbf{x}'}^{(u)}[t|t-1]\right) \quad (38)$$

$$P_{\mathbf{x},1}^{(q)}[t] := 1 - P_{\mathbf{x},0}^{(q)}[t]. \quad (39)$$

Note that, in this case, the above probabilities account for the event of users other than q suffering interference. Once these expressions have been modified, the correction step is implemented by simply substituting (38)-(39) into (35)-(37).

V. Numerical results

Consider the scenario depicted in Fig. 1, where $M = 12$ SU transceivers (marked with green circles) are deployed over an area of 400×400 m and cooperate in routing packets to the sink node U_{12}. One data flow is simulated, and traffic is generated at SUs $\mathcal{N}_S := \{1, 2, 3, 4, 7, 8\}$. A PU transmitter (marked with a purple triangle) communicates with 2 PU receivers (purple rhombus) using a power of 3 dB. The first PU receiver is located at $\mathbf{x}^{(1)} = (x = 250, y = 280)$, static, and it is served by the PU source during the entire simulation interval $t \in [1, 10^4]$. The second PU is located at $\mathbf{x}^{(2)} = (130, 240)$, mobile, with $\phi_{\mathbf{x},\mathbf{x}'}^{(q)}[t] = 0.05\ \forall \mathbf{x}' \in \mathcal{G}_{\mathbf{x}}$, and it is served by the PU source only during the interval $[1, 5 \times 10^3]$. The PU system is protected by setting $I = -70$ dB and $i^{\max} = 0.05$. The path loss obeys the model $\gamma_{m,\mathbf{x}} = \|\mathbf{x}_m - \mathbf{x}\|_2^{-3.5}$, while a Rayleigh-distributed small-scale fading is simulated [20].

From the sensing phase, the SU system can acquire an estimate of the PU source location, and of its coverage region (see, e.g., [11]–[13]). The PU coverage region is then discretized

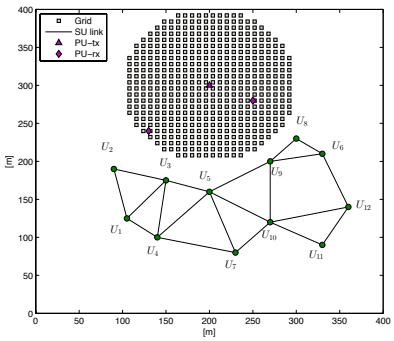

Fig. 1. Simulated scenario.

using uniformly spaced grid points (marked with gray squares in Fig. 1), each one covering an area of 8×8 m. To assess robustness to model mismatches, it is assumed that: *i)* the SUs have imperfect knowledge of the PU transition probabilities, which are supposed to be $\hat{\phi}^{(q)}_{\mathbf{x},\mathbf{x}'} = 0.01$ for both receivers; and, *ii)* when the system-wide interference notification strategy is adopted (see Section IV-B), the presumed number of PUs is always $Q = 2$, even in the interval $[5 \times 10^3, 10^4]$ where only one PU receiver is present. The multipliers are initialized as $\lambda^k_m[0] = 0.1$, $\pi_m[0] = 0.03$, and $\theta[0] = 40$, while the stepsizes are set to $\mu_\lambda = 0.5$, $\mu_\pi = 0.03$, and $\mu_\theta = 0.3$.

The (performance of the) proposed RA is compared with:

s1) an approach where the beliefs are set to 1 for grid points on the boundary of the PU coverage region [10], [13], [14]; and,

s2) a scheme where perfect PSI (including that of SU-to-PU instantaneous channels) is available.

Clearly, s2 represents an unrealistic scenario, but it serves as a benchmark to assess the performance loss incurred by the lack of full SU-PU coordination. For strategies *s1*-*s2*, $\theta[0]$ is set to 5. A normalized bandwidth $W = 1$ is considered; hence, instantaneous and average rates are expressed in bit/s/Hz. All nodes $\mathcal{N}_S$ generate best-effort traffic ($a^{1,\min}_m = 0$), with a maximum average rate of $a^{1,\max}_m = 1$ bit/s/Hz. Utility and cost functions are $V^k_m = \log_2(a^k_m)$ and $J_m(\bar{p}_m) = \bar{p}^2_m$, respectively, while the coding SINR gap is set to $\kappa_m = 1$ for all U_m.

To highlight the benefits of the PU receiver maps, the total average exogenous rate $\bar{a}[t] := (1/t) \sum_{m \in \mathcal{N}_S} \sum^t_{\tau=1} a^1_m[\tau]$ achieved by the proposed joint RA and receiver map algorithm is depicted in the upper subplot of Fig. 2, and it is compared with the ones obtained by *s1* and

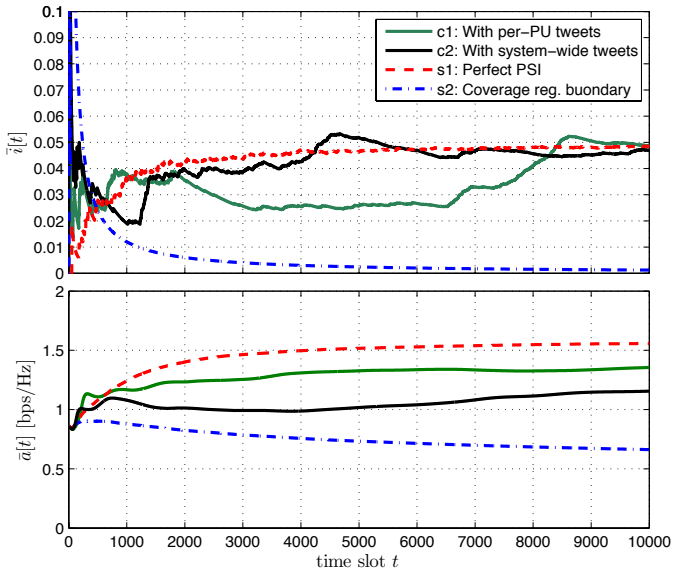

Fig. 2. Convergence of average exogenous rates and average interference.

s2. As expected, higher average rates can be obtained when perfect CSI and PSI are available. On the other hand, the proposed scheme markedly outperforms *s1*, thus justifying the additional complexity required to implement the Bayesian map estimator. The strategy based on a system-wide interference notification leads to moderately worse performance of the SU system compared to the case where per-PU receiver tweets $i^{(q)}[t]$ are broadcasted. This is however not surprising, since the strategy *(c1)* benefits from additional information on the PU system (i.e., the PU receiver that was interfered).

To further corroborate convergence and feasibility of the proposed RA scheme, the running average of the interference $\bar{i}[t] := (1/t)\sum_{\tau=1}^{t} i[\tau]$ is reported in the lower subplot of Fig. 2. It can be clearly seen that the average interference constraints are enforced when both the proposed and benchmark *s2* algorithms are utilized. On the other hand, *s1* results in an over-conservative approach. This is because the instantaneous probabilities of interference in this case are computed based on the worst-case assumption that receivers are located on the boundary of the PU coverage region, and thus the actual rate of interference is far less than expected.

Pictorially, performance of the receiver localization scheme can be assessed through the maps shown in Fig. 3 (strategy *c1*) and Fig. 4 (strategy *c2*). The value (color) of a point in the map

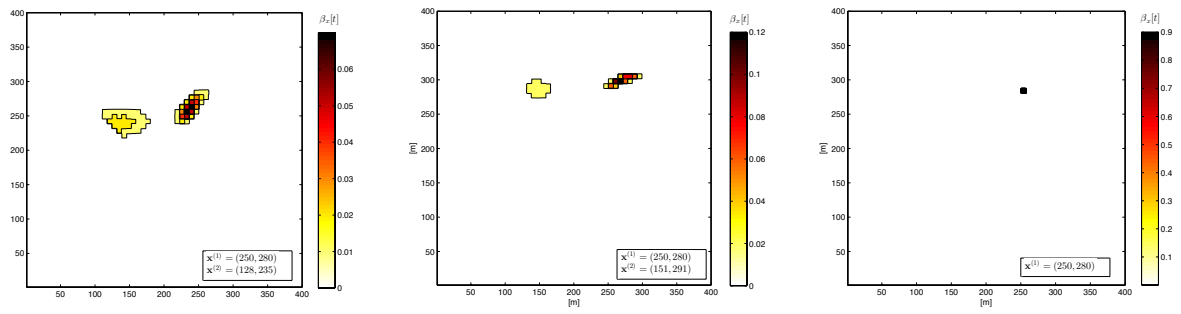

(a) (b) (c)

Fig. 3. Per-PU interference tweet: map of the sum-belief $\beta_{\mathbf{x}}[t]$ per grid point $\mathbf{x}$. (a) $t = 100$; (b) $t = 1000$; (c) $t = 6000$.

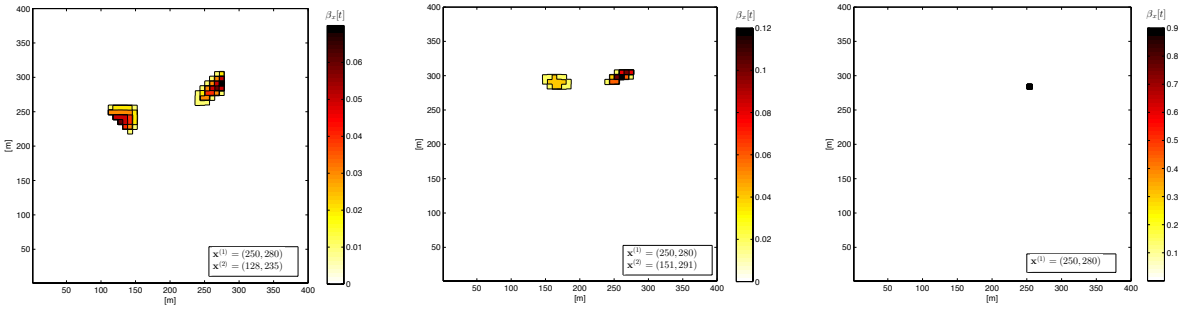

(a) (b) (c)

Fig. 4. System-wide interference notification: map of the sum-belief $\beta_{\mathbf{x}}[t]$ per grid point $\mathbf{x}$. (a) $t = 100$; (b) $t = 1000$; (c) $t = 6000$.

represents the sum of the beliefs $\beta_{\mathbf{x}}[t] := \sum_q \beta_{\mathbf{x}}^{(q)}[t|t]$ at the corresponding grid point $\mathbf{x}$. The chromatic scale uses white for low (belief) values and red for high ones. For *(c1)*, a uniform distribution across the entire PU coverage region is used for both $\beta_{\mathbf{x}}^{(1)}[0|0]$ and $\beta_{\mathbf{x}}^{(2)}[0|0]$. On the other hand, for *(c2)*, a uniform distribution across the south-east and the south-west quarters of the PU coverage region are used for $\beta_{\mathbf{x}}^{(1)}[0|0]$ and $\beta_{\mathbf{x}}^{(2)}[0|0]$, respectively. Maps in Figs. 3 (a), (b), and (c) are acquired at $t = 100$, $t = 1000$, and $t = 6000$, respectively. It can be seen that after 100 time slots, it is already possible to unveil the areas where PU receivers are likely to reside. Clearly, as time goes by, the localization accuracy improves as corroborated by Figs. 3(b) and (c). Remarkably, the PU receiver is perfectly localized in Fig. 3(c).

Recall that only one PU receiver is served by the PU source when $t > 5 \times 10^3$. Indeed, in the

TABLE I

CASE *(c1)*: AVERAGE EXOGENOUS RATES [BIT/S/HZ] FOR DIFFERENT DIMENSIONS OF THE GRID POINT (GP) [METER].

GP	$\bar{a}_1^1$	$\bar{a}_2^1$	$\bar{a}_3^1$	$\bar{a}_4^1$	$\bar{a}_7^1$	$\bar{a}_8^1$	$\sum_i \bar{a}_i^1$
3	0.181	0.138	0.181	0.190	0.289	0.281	1.541
5	0.161	0.130	0.157	0.173	0.304	0.301	1.507
7	0.169	0.137	0.150	0.182	0.299	0.272	1.470
9	0.157	0.150	0.136	0.174	0.298	0.263	1.459
15	0.151	0.149	0.139	0.153	0.250	0.190	1.309

TABLE II

CASE *(c2)*: AVERAGE EXOGENOUS RATES [BIT/S/HZ] FOR DIFFERENT DIMENSIONS OF THE GRID POINT (GP) [METER].

GP	$\bar{a}_1^1$	$\bar{a}_2^1$	$\bar{a}_3^1$	$\bar{a}_4^1$	$\bar{a}_7^1$	$\bar{a}_8^1$	$\sum_i \bar{a}_i^1$
3	0.174	0.127	0.154	0.182	0.314	0.324	1.275
5	0.176	0.157	0.163	0.186	0.296	0.273	1.248
7	0.161	0.168	0.167	0.180	0.284	0.243	1.204
9	0.167	0.148	0.175	0.177	0.313	0.260	1.240
15	0.159	0.143	0.182	0.169	0.265	0.268	1.187

setup *(c2)*, the beliefs peak at the actual location of the PU receiver, as shown in Fig. 4(c). The numerical results reveal that the two beliefs $\beta_{\mathbf{x}}^{(1)}[t|t]$ and $\beta_{\mathbf{x}}^{(2)}[t|t]$ are (approximately) the same for all $\mathbf{x}$, thus indicating that just an upper bound on Q is sufficient to carry out the receiver localization task.

Resolution of the grid $\mathcal{G}$ clearly affects the receiver localization accuracy; at the expense of an higher computational burden, finer grids allow the SU system to pinpoint the receivers' locations with higher accuracy [11]. This, is turn, influences also the RA performance, as verified by Table I. Specifically, Table I reports the running average rates $\bar{a}_i^1 := (1/t)\sum_\tau a_i^1[\tau]$, $\forall\ i \in \mathcal{N}_S$ at time $t = 5\times 10^3$, along with the overall rate $\bar{a}^1 := \sum_{i\in\mathcal{N}_S} \bar{a}_i^1$. A per-PU interference notification strategy is implemented. It can be seen that the total rate $\bar{a}^1$ increases as the grid becomes more dense. Users U_7 and U_8 achieve higher traffic rates, since they are just two hops away from the destination; this can be observed also in Table III, where the same results are reported for

TABLE III

CASES *(s1)* AND *(s2)*: AVERAGE EXOGENOUS RATES [BIT/S/HZ].

	$\bar{a}_1^1$	$\bar{a}_2^1$	$\bar{a}_3^1$	$\bar{a}_4^1$	$\bar{a}_7^1$	$\bar{a}_8^1$	$\sum_i \bar{a}_i^1$
s1	0.128	0.077	0.059	0.139	0.256	0.066	0.725
s2	0.184	0.163	0.206	0.203	0.317	0.469	1.542

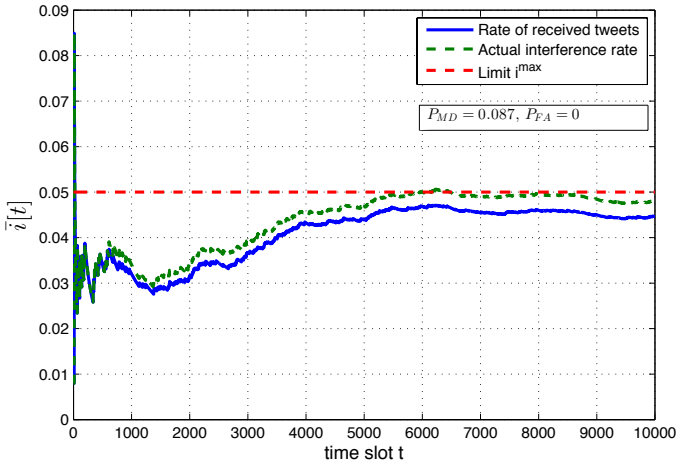

Fig. 5. Average interference rate with communication outages.

benchmark *s2*. Remarkably, when each grid point covers a 3×3 m area, the gap between the overall exogenous rates obtained with the proposed scheme, and the one with perfect CSI and PSI is of just 0.001 bit/s/Hz. Further, thanks to the receiver maps, U_8 can achieve high data rates (compared to the other SU sources) even though it is geographically close to the PU system. On the other hand, U_8 achieves an average rate one order of magnitude smaller by using the RA scheme *s1*, as shown in Table III. The average exogenous rates achieved when tweets $i[t]$ are exchanged between the systems are reported in Table II. Again, SUs attain higher rates by using a fine-grained discretization of the PU coverage region. Strategy *(c2)* leads to moderately worse performance of the SU system, and the gap with the overall rates achieved using per-PU receiver tweets $i^{(q)}[t]$ is on the same order in all the cases tested.

Next, the case where the secondary system does not correctly decode all the interference tweets is tested. Suppose that the sink node U_{12} acts as an NC for the secondary system, and assume that strategy *(c2)* is employed. The probability of outage on the communication link between

the PU transmitter and SU U_{12} is set to $P_{MD} = 0.087$, which corresponds to the probability that the instantaneous SINR at U_{12} stays below a given threshold [20]. Further, assume that each grid point covers an area of 8×8 m. The trajectory of the cumulative moving average of the interference is shown Fig. 5. Specifically, the cumulative moving average of both the actual interference and the interference tweets received are plotted. As expected, for $t > 6000$ the rate of correctly received tweets floors at a level slightly lower than $i^{\max}$. Indeed, the actual interference rate levels off at $i^{\max}$, thus protecting the PU system from excessive interference despite communication errors.

VI. Concluding remarks

Dynamic cross-layer resource allocation and user localization algorithms for an underlay multi-hop cognitive radio network were designed. A robust recursive Bayesian approach was developed to estimate (and track) the unknown location of the PU receivers. The inputs of the estimator were the (past and current) power transmitted by the secondary system, and a binary interference notification (tweet) broadcasted by the primary system. The schemes were found robust to errors on the observations and accounted for PU mobility. The estimated maps and the remaining CSI serve as input of a cross-layer optimization. In particular, the resource allocation schemes were obtained as the solution of a constrained network-utility maximization that optimized performance of the secondary network and accounted for the distinctive features of the cognitive setup, including a constraint that limited the long-term probability of interfering the primary receivers. The optimal solution dictated how to adapt the resources at different layers as a function of the perfect CSI of the SU-to-SU links and the uncertain CSI of the SU-to-PU links. Numerical results validated the novel approach and confirmed that such a minimal feedback suffices to accurately estimate (and track) the location of PU receivers.

Appendix: Proof of Propositions 3 and 4

Rearranging the terms of $\mathcal{L}(\mathcal{Y}, \mathbf{d}^*)$ and isolating those dependent on $\{r^k_{m,n}[t]\}$, $\{w_{m,n}[t]\}$, and $\{p_{m,n}[t]\}$, we have that $\mathbb{E}_{\mathbf{g},\mathbf{s}}[\sum_{(m,n)\in\mathcal{E}}[\sum_k r^k_{n,m}\lambda^{k*}_{m,n} - \pi^*_m w_{m,n}p_{m,n} - \theta^* w_{m,n} i_{m,n}(p_{m,n})]]$. Clearly, the latter is separable per-fading state. Hence, maximizing the Lagrangian amounts to solving,

per fading state, the problem

$$\max_{\{r^k_{m,n},w_{m,n},p_{m,n}\}} \sum_{(m,n)\in\mathcal{E}} \Big[\sum_k r^k_{n,m}\lambda^{k*}_{m,n} - \pi^*_m w_{m,n}p_{m,n} - \theta^* w_{m,n}\mathbb{E}_{\mathbf{s}[t]}[i_{m,n}(p_{m,n})]\Big] \tag{40a}$$

$$\text{s.to } \sum_k r^k_{n,m} \le w_{m,n}C_{m,n}(\mathbf{g}[t],p_{m,n})\,,\forall\,(m,n)\in\mathcal{E} \tag{40b}$$

$$\sum_{(m,n)\in\mathcal{E}} w_{m,n}\le 1,\; p_{m,n}\in[0,p^{\max}_m],\; w_{m,n}\in[0,1], \tag{40c}$$

where the constraints not dualized have been written explicitly.

Consider first solving (40) w.r.t. $\{r^k_{m,n}\}$. Per link (m,n), and for any given value of $w_{m,n}$ and $p_{m,n}$, rates $r^{k*}_{m,n}\ge 0$ are obtained by maximizing a linear function over a simplex. Thus, the optimal arguments $r^{k*}_{m,n}$ will lie on the boundary of the constraints. Recall that $\lambda^*_{m,n}=\max_k\lambda^{k*}_{m,n}$ and define $\mathcal{K}_{m,n}:=\{k:\lambda^*_{m,n}=\lambda^{k*}_{m,n}\}$. Then, it is straightforward to show that: i) if $\lambda^{k*}_{m,n}\le 0$, then $r^{k*}_{m,n}=0$ for all k; and if $\lambda^{k*}_{m,n}>0$, then $r^{k*}_{m,n}=0$ for $k\notin\mathcal{K}_{m,n}$ and $\sum_{k\in\mathcal{K}_{m,n}} r^k_{n,m}=w_{m,n}C_{m,n}(\mathbf{g}[t],p_{m,n})$. This is in fact, the main result in Proposition 4. As a special case, when all weights $\lambda^{k*}_{m,n}$ are different, one has the "winner-takes-all" solution (21).

After substituting $\{r^{k*}_{m,n}\}$ into (40a), one can drop constraint (40b) and replace $\sum_k r^k_{n,m}\lambda^{k*}_{m,n}$ with $\sum_{\mathcal{K}_{m,n}} r^k_{n,m}\lambda^*_{m,n}$ and the latter with $w_{m,n}C_{m,n}(\mathbf{g}[t],p_{m,n})\lambda^*_{m,n}$. Hence, the optimum $\{w^*_{m,n}\}$, and $\{p^*_{m,n}\}$ are found by solving

$$\max_{\{w_{m,n},p_{m,n}\}} \sum_{(m,n)\in\mathcal{E}} \Big[w_{m,n}C_{m,n}(\mathbf{g}[t],p_{m,n})\lambda^*_{m,n} - \pi^*_m w_{m,n}p_{m,n} - \theta^* w_{m,n}\mathbb{E}_{\mathbf{s}[t]}[i_{m,n}(p_{m,n})]\Big] \tag{41a}$$

$$\text{s.to } \sum_{(m,n)\in\mathcal{E}} w_{m,n}\le 1\,,\; p_{m,n}\in[0,p^{\max}_m],\; w_{m,n}\in[0,1]. \tag{41b}$$

Recall that the definition of the link-quality indicator is [cf. (17)] $\varphi_{m,n}(\mathbf{g}[t],p_{m,n}) = \lambda^*_{m,n}$ $C_{m,n}(\mathbf{g}[t],p_{m,n})-\pi^*_m w_{m,n}p_{m,n}-\theta^* w_{m,n}\mathbb{E}_{\mathbf{s}[t]}[i_{m,n}(p_{m,n})]$. Then, (41a) can be rewritten as

$$\max_{\{w_{m,n},p_{m,n}\}} \sum_{(m,n)\in\mathcal{E}} w_{m,n}\varphi_{m,n}(\mathbf{g}[t],p_{m,n})\,. \tag{42}$$

It is then clear that: i) for any value of $w_{m,n}$, the optimal power can be found separately as $p^*_{m,n}=\arg\max_{p_{m,n}}\ \varphi_{m,n}(\mathbf{g}[t],p_{m,n})$ s. to $p_{m,n}\in[0,p^{\max}_m]$; and ii) the optimal scheduling coefficients are found as $w^*_{m,n}=\arg\max_{\{w_{m,n}\}}\sum_{(m,n)\in\mathcal{E}} w_{m,n}\varphi_{m,n}(\mathbf{g}[t],p^*_{m,n})$ s. to $w_{m,n}\in[0,1]$ and $\sum_{(m,n)\in\mathcal{E}} w_{m,n}\le 1$. Clearly, this is a linear program and its solution lies on the boundary

of the constraints. Specifically, $w^*_{m,n} = 0$ unless $(m,n) = \arg\max_{m',n'} \varphi_{m',n'}(\mathbf{g}[t], p^*_{m',n'})$. These are precisely the results in Proposition 3.

REFERENCES

[1] Q. Zhao and B. M. Sadler, "A survey of dynamic spectrum access," *IEEE Sig. Proc. Mag.*, vol. 24, no. 3, pp. 79–89, May 2007.

[2] A. Ghasemi and E. S. Sousa, "Fundamental limits of spectrum-sharing in fading environments," *IEEE Trans. Wireless Commun.*, vol. 6, no. 2, pp. 649–658, Feb. 2007.

[3] Y. Chen, G. Yu, Z. Zhang, H.-H. Chen, and P. Qiu, "On cognitive radio networks with opportunistic power control strategies in fading channels," *IEEE Trans. Wireless Commun.*, vol. 7, no. 7, pp. 2752–2761, Jul. 2008.

[4] R. Zhang, "On peak versus average interference power constraints for protecting primary users in cognitive radio networks," *IEEE Trans. Wireless Commun.*, vol. 8, no. 4, pp. 2112–2120, Apr. 2009.

[5] S. Huang, X. Liu, and Z. Ding, "Decentralized cognitive radio control based on inference from primary link control information," *IEEE J. Sel. Areas Commun.*, vol. 29, pp. 394–406, Feb. 2011.

[6] X. Kang, Y.-C. Liang, A. Nallanathan, H. K. Garg, and R. Zhang, "Optimal power allocation for fading channels in cognitive radio networks: Ergodic capacity and outage capacity," *IEEE Trans. Wireless Commun.*, vol. 8, no. 2, pp. 940–950, Feb. 2009.

[7] X. Wang, "Joint sensing-channel selection and power control for cognitive radios," *IEEE Trans. Wireless Commun.*, vol. 10, no. 3, pp. 958–967, Mar. 2011.

[8] X. Gong, S. Vorobyov, and C. Tellambura, "Optimal bandwidth and power allocation for sum ergodic capacity under fading channels in cognitive radio networks," *IEEE Trans. Sig. Proc.*, vol. 59, no. 4, pp. 1814–1826, Apr. 2011.

[9] A. G. Marques, L. M. Lopez-Ramos, G. B. Giannakis, and J. Ramos, "Resource allocation for interweave and underlay cognitive radios under probability-of-interference constraints," *IEEE J. Sel. Areas Commun.*, vol. 30, no. 10, pp. 1922–1933, Nov. 2012.

[10] E. Dall'Anese, S.-J. Kim, G. B. Giannakis, and S. Pupolin, "Power control for cognitive radio networks under channel uncertainty," *IEEE Trans. Wireless Commun.*, vol. 10, no. 10, pp. 3541–3551, Dec. 2011.

[11] E. Dall'Anese, J. A. Bazerque, and G. B. Giannakis, "Group sparse Lasso for cognitive network sensing robust to model uncertainties and outliers," *Elsevier Phy. Commun.*, vol. 5, no. 2, pp. 161–172, Jun. 2012.

[12] J. Wang, P. Urriza, Y. Han, and D. Čabrić, "Weighted centroid algorithm for estimating primary user location: Theoretical analysis and distributed implementation," *IEEE Trans. Wireless Commun.*, vol. 10, no. 10, pp. 3403–3413, Oct. 2011.

[13] B. Mark and A. Nasif, "Estimation of maximum interference-free power level for opportunistic spectrum access," *IEEE Trans. Wireless Commun.*, vol. 8, no. 5, pp. 2505–2513, May 2009.

[14] E. Dall'Anese and G. B. Giannakis, "Statistical routing for multihop wireless cognitive networks," *IEEE J. Sel. Areas Commun.*, vol. 30, no. 10, pp. 1983–1993, Nov. 2012.

[15] Y. Ho and R. Lee, "A Bayesian approach to problems in stochastic estimation and control," *IEEE Trans. Auto. Contr.*, vol. 9, no. 4, pp. 333–339, Oct. 1964.

[16] V. Cevher, P. Boufounos, R. G. Baraniuk, A. C. Gilbert, and M. J. Strauss, "Near-optimal Bayesian localization via incoherence and sparsity," in *Intl. Conf. on Info. Proc. in Sensor Netw.*, San Francisco, CA, Apr. 2009, pp. 205–216.

[17] N. Patwari and A. O. Hero III, "Using proximity and quantized RSS for sensor localization in wireless networks," in *2nd ACM Intl. Conf. on Wireless Sensor Netw. and App.*, 2003, pp. 20–29.

[18] K. Eswaran, M. Gastpar, and K. Ramchandran, "Bits through ARQs: Spectrum sharing with a primary packet system," in *in Proc. of IEEE Intl. Symp. on Info. Theory*, Nice, France, Jun. 2007, see also: `http://arxiv.org/pdf/0806.1549.pdf`.

[19] A. G. Marques, L. M. Lopez-Ramos, G. B. Giannakis, J. Ramos, and A. Caamano, "Resource allocation for interweave and underlay cognitive radios under probability-of-interference constraints," *IEEE Trans. Veh. Technol.*, vol. 61, no. 6, pp. 2789 – 2807, Jul. 2012.

[20] A. Goldsmith, *Wireless communications*. Cambridge University Press, 2005.

[21] E. Dall'Anese, S.-J. Kim, and G. B. Giannakis, "Channel gain map tracking via distributed Kriging," *IEEE Trans. Veh. Technol.*, vol. 60, no. 3, pp. 1205–1211, Mar. 2011.

[22] L. Georgiadis, M. J. Neely, and L. Tassiulas, "Resource allocation and cross-layer control in wireless networks," *Found. Trends in Networking*, vol. 1, no. 1, pp. 1–144, 2006.

[23] Y.-J. Chang, F.-T. Chien, and C.-C. Kuo, "Cross-layer QoS analysis of opportunistic OFDM-TDMA and OFDMA networks," *IEEE J. Sel. Areas Commun.*, vol. 25, no. 4, pp. 657–666, May 2007.

[24] T. Yoo and A. Goldsmith, "Capacity and power allocation for fading mimo channels with channel estimation error," *IEEE Trans. Info. Theory*, vol. 52, no. 5, pp. 2203–2214, May 2006.

[25] A. Ribeiro and G. B. Giannakis, "Separation principles in wireless networking," *IEEE Trans. Info. Theory*, vol. 56, no. 9, pp. 4488–4505, Sep. 2010.

[26] L. Chen, S. H. Low, M. Chiang, and J. C. Doyle, "Cross-layer congestion control, routing and scheduling design in ad hoc wireless networks," in *Proc. of IEEE INFOCOM*, Barcelona, Spain, Apr. 2006.

[27] X. Lin and N. B. Shroff, "The impact of imperfect scheduling on cross-layer congestion control in wireless networks," *IEEE/ACM Trans. on Netw.*, vol. 14, no. 2, pp. 302–315, Apr. 2006.

[28] A. G. Marques, , X. Wang, and G. B. Giannakis, "Dynamic resource management for cognitive radios using limited-rate feedback," *IEEE Trans. Sig. Proc.*, vol. 57, no. 9, pp. 3651–3666, Sep. 2009.

[29] A. Ribeiro, "Ergodic stochastic optimization algorithms for wireless communication and networking," *IEEE Trans. Sig. Proc.*, vol. 58, no. 12, pp. 6369–6386, Dec. 2010.

[30] D. Bertsekas, A. Nedic, and A. E. Ozdaglar, *Convex Analysis and Optimization*. Athena Scientic, 2003.

Cross-Layer Optimization and Receiver Localization for Cognitive Networks Using Interference Tweets

Antonio G. Marques, Emiliano Dall'Anese, and Georgios B. Giannakis

***Abstract*—A cross-layer resource allocation scheme for underlay multi-hop cognitive radio networks is formulated, in the presence of *uncertain* propagation gains *and* locations of primary users (PUs). Secondary network design variables are optimized under long-term probability-of-interference constraints, by exploiting channel statistics and maps that pinpoint areas where PU receivers are likely to reside. These maps are tracked using a Bayesian approach, based on 1-bit messages - here refereed to as "interference tweet" - broadcasted by the PU system whenever a communication disruption occurs due to interference. Although nonconvex, the problem has zero duality gap, and it is optimally solved using a Lagrangian dual approach. Numerical experiments demonstrate the ability of the proposed scheme to localize PU receivers, as well as the performance gains enabled by this minimal primary-secondary interplay.**

***Index Terms*—Wireless cognitive radio networks, cross-layer optimization, receiver localization, Lagrange dual, Bayesian estimation.**

I. Introduction

In an hierarchical spectrum access mode, underlay cognitive radios (CRs) can opportunistically (re-)use the frequency bands licensed to a primary user (PU) system, provided ongoing primary communications are not overly disrupted [1]. Once spectral opportunities are identified through sensing, control of the interference inflicted to incumbent users is crucial to enable a seamless coexistence of primary and CR-empowered secondary systems [2]–[5].

As in conventional wireless networking, knowledge of the propagation gains is instrumental to controlling the co-channel interference. However, since the PU system has generally no incentive to exchange synchronization and channel training signals with secondary users (SUs), SU-to-PU channels are difficult to acquire in practice. In lieu of instantaneous propagation gains, the *distribution* of the PU-to-SU channels can be used to limit the instantaneous interference inflicted to PUs by means of average or probabilistic constraints [2]–[10]. Power control for underlay CRs under channel uncertainty was considered in, e.g., [2], [3], for one PU link and one SU link. Instantaneous and average interference constraints were compared in [4] for the same setup, while an extension to multiple SU links can be found in e.g., [6]–[9].

State-of-the-art spectrum sensing schemes can detect and localize active PU *sources* [11]–[13], but not "passive" PU *receivers*, which may remain silent most of the time. Since localization based on received signal strength (RSS) measurements over (short) primary signalling messages such as e.g., (re)transmissions requests, is challenging (and these messages may be exchanged over a primary control channel), knowledge of the PU receiver locations must be assumed uncertain. A prudent alternative to bypass the need to gather information about the PU receivers' locations is to estimate the PU coverage region [11], [13], and ensure that the interference does not exceed a prescribed level at any point of the coverage region boundary [10], [13], [14]. However, this conservative approach leads to a sub-optimal operation of the SU network, especially when PU receivers are not close to the boundary. The alternative is to account for the uncertainty in the receivers location, which indirectly generates uncertainty on the gains of the SU-to-PU channels. This calls for schemes that use the available information to infer the location of the PU receivers, and account for channel state information (CSI) imperfections present in the overall network optimization procedure.

The present paper advocates the novel notion of *receiver map* as a tool for unveiling areas where PU receivers are located, with the objective of limiting the interference inflicted to those locations. These maps are tracked using a recursive Bayesian estimator [15], which is based on a 1-bit message broadcasted by the PU system whenever the instantaneous interference inflicted to a PU receiver exceeds a given tolerable level. These simple interference announcements are reminiscent of modern real-time social messaging systems - thus, the term "interference tweets" - and puts the hierarchical spectrum access paradigm closer to a community-based wireless networking setup. Two broadcasting setups are considered. In the first one, a binary interference announcement is sent by e.g., a base station or a primary network controller (NC); in this message, no information regarding the PU(s) that was (were) interfered is provided. In the second case, the number of PUs interfered and their identities are known; this is because this information is specified in the tweet sent by the primary NC (requiring a few additional bits to indicate the interfered PUs), or, because the PU receivers sent the tweet themselves (and the PU identifier is included as usual in the packet header). The case where the interference tweet is not correctly received by the SU system due to e.g., deep fading, is also analyzed. Bayesian localization using quantized RSS measurements was considered in e.g., [16], [17]. Instead of RSS samples, areas

Submitted: March 27, 2013

This work was supported by the QNRF grant NPRP 09-341-2-128. A. G. Marques is with the Dep. of Signal Theory and Communications, Universidad Rey Juan Carlos, Camino del Molino s/n, Fuenlabrada, Madrid 28943, Spain. E. Dall'Anese and G. B. Giannakis are with the Digital Technology Center and the Dept. of ECE, University of Minnesota, 200 Union Street SE, Minneapolis, MN 55455, USA. E-mails: antonio.garcia.marques@urjc.es, {emiliano, georgios}@umn.edu. Part of this work was submitted to the *38th IEEE Intl. Conf. on Acoustics, Speech and Signal Processing*, Vancouver, Canada, May 2013, and to the *14th IEEE Intl. Workshops on Sig. Proc. Advances for Wireless Commun*, Darmstadt, Germany, June 2013.

where PU receivers are likely to reside are unveiled here by exploiting the PU interference tweets and the distribution of SU-to-PU propagation gains.

In the mainstream CR literature, SUs are de facto envisioned to gain access to licensed frequencies without requiring any modification to communication and operational protocols of primary systems. Requiring the PU system to broadcast one bit when disruptive interference occurs, involves a slight modification of the primary system operation. However, it will be shown that significant improvements in spectrum (re)use efficiency can be obtained with this minimal system interplay, thus reaping off the benefits offered by the CR technology to the full extent. In setups where the broadcasting of tweets is not feasible, the secondary network can still estimate the receiver map by e.g., overhearing retransmission requests of the PUs [5], [18]. The schemes designed in this paper can be naturally extended to account for this sensing mode, thanks to their ability to handle uncertain/erroneous interference notifications; however, map estimation accuracy and overall performance of the secondary network certainly deteriorate relative to the case where tweets are broadcasted.

Similar to [9], [19], the proposed cross-layer resource allocation (RA) scheme is designed as the solution of a constrained optimization problem featuring long-term probability-of-interference constraints. Specific to the present formulation is the the presence of uncertain SU-to-PU propagation gains *and* uncertain locations of PUs, as well as a multi-hop secondary network setup. Access among SUs is assumed orthogonal, and the resources at the transport, network, link and physical layers are adapted to the *time-varying* SU-to-SU *channels and* the receiver *maps*. Although nonconvex, the formulated problem has zero duality gap, and it is optimally solved using a Lagrangian dual approach. Taking advantage of the problem separability across SUs in the dual domain, computationally-affordable optimal solvers for transmit-powers, scheduling and routing variables, as well as exogenous traffic rates are developed.

The rest of the paper is organized as follows. System model and problem formulation are presented in Section II. The RA is solved optimally in Section III. Section IV presents the receiver map machinery. Numerical experiments are provided in Section V, and Section VI concludes the paper.[1]

II. Modeling and Problem formulation

A. Primary and secondary state information

Consider a multi-hop SU network comprising M nodes $\{U_m\}_{m=1}^M$ deployed over an area $\mathcal{A} \subset \mathbb{R}^2$. Assume that SUs share a flat-fading frequency band with an incumbent PU system in an underlay setup [1]; though, methods and results presented throughout the paper can be readily extended to multiple (frequency-selective) bands. Based on the output of the spectrum sensing stage [11]–[13], SUs implement adaptive RA to maximize network performance, while protecting the PU system from excessive interference.

When spectral resources are shared in a hierarchical setup, the channel state information (CSI) available to the SU network is heterogeneous; in fact, the accuracy of the CSI for a given link typically depends on whether PUs or SUs are involved [2]. Provided the spectrum is available for the SUs to transmit, the SU-to-SU channels can be readily acquired by employing conventional training-based channel estimators. For this reason, the state of the SU-to-SU channels is considered known. The instantaneous gain of link $U_m \to U_n$ is denoted as $g_{m,n}$, and it is given by the squared magnitude of the small-scale fading realization scaled by the average signal-to-interference-plus-noise ratio (SINR) [20], so that it accounts also for the interference inflicted to SUs by the PU sources.

Suppose now that PU transmitters communicate with Q PU *receivers* geolocated at $\{\mathbf{x}^{(q)} \in \mathcal{A}\}_{q=1}^Q$, and denote by $h_{m,\mathbf{x}^{(q)}}$ the instantaneous channel gain between U_m and position $\mathbf{x}^{(q)}$. Since PUs have generally no incentive to use primary spectral resources to exchange synchronization and channel training signals with SUs [1], training-based channel estimation cannot be employed at the SU end to acquire $\{h_{m,\mathbf{x}^{(q)}}\}$. Thus, even though the *average link gain* can be obtained based on locations $\{\mathbf{x}^{(q)} \in \mathcal{A}\}_{q=1}^Q$ [20], the instantaneous value of the primary link is *uncertain* due to random fast fading effects. Consequently, SU m cannot assess precisely the interference that it will cause to PU q. Hereafter, it is assumed that only the joint distribution of processes $\{h_{m,\mathbf{x}^{(q)}}\}$ is known to the SU network, which is denoted as $\phi_h(\{h_{m,\mathbf{x}^{(q)}}\})$. Thus, given the maximum instantaneous interference power I tolerable by the PUs, the secondary network can determine the interference probabilities at each location $\mathbf{x}^{(q)}$. For instance, in an orthogonal access mode, if U_m is scheduled to access the channel with a transmit-power p, the probability of causing interference to PU receiver q is $\Pr\left\{p\, h_{m,\mathbf{x}^{(q)}} > I\right\}$.

Acquiring the location of passive PU receivers is challenging because conventional spectrum sensing schemes aim to detect and localize active PU *sources* [11]–[13]. PU receivers remain silent most of the time, and their signalling messages may not be easily detected (especially if they are sent over a dedicated control channel). As a consequence, locations $\{\mathbf{x}^{(q)} \in \mathcal{A}\}_{q=1}^Q$ are generally *uncertain*. Let $z_{\mathbf{x}}^{(q)}$ be a binary variable taking the value 1 if PU receiver q is located at $\mathbf{x} \in \mathcal{A}$. Further, consider discretizing the PU coverage region into a set of grid points $\mathcal{G} := \{\mathbf{x}_g\}$ representing *potential* locations for the PU receivers. In lieu of $\{z_{\mathbf{x}}^{(q)}\}$, the idea here is to use the probabilities $\beta_{\mathbf{x}}^{(q)} := \Pr\{z_{\mathbf{x}}^{(q)} = 1\}$, $\forall\, \mathbf{x} \in \mathcal{G}$, to identify areas where a PU receiver q is more likely to reside, and limit the interference accordingly. To this end, the following is assumed.

(as1) $\{g_{m,n}\}$ and $\{h_{m,\mathbf{x}^{(q)}}\}$ are mutually independent; and,

(as2) $z_{\mathbf{x}}^{(q)}$ and $z_{\mathbf{x}}^{(v)}$, with $q \neq v$, are independent.

Assumption *(as2)* presupposes that each PU receiver has its own mobility pattern, while *(as1)* implies that the uncertainty of $\{h_{m,\mathbf{x}^{(q)}}\}$ is spatially uncorrelated. This is certainly the case

[1] *Notation:* $\mathbb{E}_{\mathbf{g}}[\cdot]$ denotes expectation with respect to (w.r.t.) the random process $\mathbf{g}$; $\Pr\{A\}$ the probability of event A; x^* the optimal value of x; $\mathbb{1}_{\{\cdot\}}$ the indicator function ($\mathbb{1}_{\{x\}} = 1$ if x is true, and zero otherwise); $[x]_+$ the projection of the scalar x onto the non-negative outhunt; and, $[x]_a^b := \min\{\max\{x, a\}, b\}$ the projection of the scalar x onto $[a, b]$. Given a function $V(x)$, $\dot{V}(x)$ denotes the derivative function or the derivative of $V(x)$, and $(V)^{-1}(x)$ the inverse function, provided it exists. Finally, $\wedge$ denotes the "and" logical operator.

when, e.g., spatial correlation of shadowing is negligible [5], [13], or path loss and shadowing are accurately acquired as in e.g., [21]. Next, sets $\mathbf{g} := \{g_{m,n}\}$ and $\mathbf{s} := \{\phi_h\} \cup \{\beta_{\mathbf{x}}^{(q)}\}$ collect the available secondary CSI, and the statistical primary state information (PSI), respectively.

B. RA under primary state uncertainty

Application-level data packets are generated exogenously at the SUs, and routed throughout the network to the intended destination(s). Packet streams are referred to as flows, and they are indexed by k. The destination of each flow is denoted by $d(k)$. Different traffic flows (e.g., video, voice, or elastic data) may be generated at the same SU, and routed towards the same destination. For each flow k, packet arrivals at U_m are modeled by a stationary stochastic process with mean $a_m^k \geq 0$.

Let $r_{m,n}^k(\mathbf{g},\mathbf{s}) \geq 0$ be the instantaneous rate used for routing packets of flow k on link $U_m \rightarrow U_n$, during the state realizations $\mathbf{g}$ and $\mathbf{s}$. Suppose that SUs are equipped with queues (buffers) to store all incoming packets (exogenous and endogenous), so that no packets are discarded. Let $b_m^k[t]$ denote the amount of packets of flow k that at time t are stored in the queue of node m. In this paper, queues are deemed stable if $\lim_{t\rightarrow+\infty}(1/t)\sum_{\tau=1}^{t}\mathbb{E}[b_m^k[\tau]] < \infty$ [22]. Accordingly, for queues to be stable, exogenous and endogenous rates need to satisfy the following necessary condition for all m and k:

$$a_m^k + \sum_{n\in\mathcal{N}_m}\mathbb{E}_{\mathbf{g},\mathbf{s}}\left[r_{n,m}^k(\mathbf{g},\mathbf{s})\right] \leq \sum_{n\in\mathcal{N}_m}\mathbb{E}_{\mathbf{g},\mathbf{s}}\left[r_{m,n}^k(\mathbf{g},\mathbf{s})\right] \quad \forall\, m \neq d(k) \tag{1}$$

where $\mathcal{N}_m \subset \{1,\ldots,M\}$ denotes the set of one-hop neighboring nodes of U_m. SUs implement flow control, and thus the rates $\{a_m^k\}$ will be variables of the RA problem. Clearly, $\{\mathbb{E}_{\mathbf{g},\mathbf{s}}[r_{m,n}^k]\}_{n\in\mathcal{N}_m}$ specify the average amount of packets that are routed through each of the U_m's outgoing links.

As for the medium access layer, define a binary scheduling variable $w_{m,n}$ taking the value 1 if U_m is scheduled to transmit to its neighbor U_n, and 0 otherwise. Secondary transmissions are assumed orthogonal. Orthogonal access is adopted by a gamut of wireless systems because of its low-complexity implementation. It also enables a (nearly) optimal network operation under moderate-to-strong interference transmission scenarios [23]. Assuming that one secondary link is scheduled per time slot, it follows that

$$\sum_{(m,n)\in\mathcal{E}} w_{m,n}(\mathbf{g},\mathbf{s}) \leq 1 \tag{2}$$

where $\mathcal{E} := \{(m,n) : n \in \mathcal{N}_m, m = 1,\ldots,M\}$ represents the set of SU-to-SU links. When $\sum_{(m,n)\in\mathcal{E}} w_{m,n}(\mathbf{g},\mathbf{s}) = 0$, no SU transmits because either the quality of all SU-to-SU channels is poor, or, excessive interference is inflicted to PUs.

At the physical layer, instantaneous rate and transmit power variables are coupled, and this rate-power coupling is modeled here using Shannon's capacity formula $C_{m,n}(g_{m,n},p_{m,n}) = W\log(1+p_{m,n}g_{m,n}/\kappa_{m,n})$, where $\kappa_{m,n}$ represents the coding scheme-dependent SINR gap [20], and W is the bandwidth of the primary channel that is to be (re-)used. The premise for this capacity formula is that channels $\{g_{m,n}\}$ can be estimated perfectly. Notice however that errors in the estimation of $\{g_{m,n}\}$ can be readily accounted for as shown in, e.g., [24]. Let $\bar{p}_m$ denote the average transmit-power of U_m, which can be expressed as

$$\bar{p}_m = \mathbb{E}_{\mathbf{g},\mathbf{s}}\left[\sum_{n\in\mathcal{N}_m} w_{m,n}(\mathbf{g},\mathbf{s})p_{m,n}(\mathbf{g},\mathbf{s})\right]. \tag{3}$$

Power transmitted by the SUs have to obey two different constraints. First, due to spectrum mask specifications, the instantaneous power $p_{m,n}$ cannot exceed a pre-defined limit $p_m^{\max}$. Second, the average power satisfies $\bar{p}_m \leq \bar{p}_m^{\max}$.

To account for the interference inflicted to the PU system [1], define the binary variable $i^{(q)}(\{p_{m,n}\},\mathbf{s})$ as

$$i^{(q)}(\{p_{m,n}\},\mathbf{s}) := \sum_{\mathbf{x}\in\mathcal{G}} \mathbb{1}_{\{\sum_{(m,n)\in\mathcal{E}} w_{m,n}(\mathbf{g},\mathbf{s})p_{m,n}(\mathbf{g},\mathbf{s})h_{m,\mathbf{x}^{(q)}} > I\}} z_{\mathbf{x}}^{(q)}. \tag{4}$$

Since $z_{\mathbf{x}}^{(q)}$ pinpoints the location of PU receiver q, variable $i^{(q)}(\{p_{m,n}\},\mathbf{s})$ clearly indicates whether or not excessive instantaneous interference is inflicted to PU receiver q. Further, define the binary random variable

$$i(\{p_{m,n}\},\mathbf{s}) := 1 - \prod_{q=1}^{Q}(1 - i^{(q)}(\{p_{m,n}\},\mathbf{s})), \tag{5}$$

which is 1 if one or more PU receivers are interfered. Since $w_{m,n}(\mathbf{g},\mathbf{s}) \in \{0,1\}$, and at most one secondary link is active per time slot, $i(\{p_{m,n}(\mathbf{g},\mathbf{s})\},\mathbf{s})$ can be equivalently rewritten as

$$i(\{p_{m,n}(\mathbf{g},\mathbf{s})\},\mathbf{s}) = \sum_{(m,n)\in\mathcal{E}} w_{m,n}(\mathbf{g},\mathbf{s})i_{m,n}(p_{m,n}(\mathbf{g},\mathbf{s}),\mathbf{s}) \tag{6}$$

where

$$i_{m,n}(p,\mathbf{s}) := 1 - \prod_{q=1}^{Q}\left(1 - \sum_{\mathbf{x}\in\mathcal{G}} \mathbb{1}_{\{ph_{m,\mathbf{x}^{(q)}} > I\}} z_{\mathbf{x}}^{(q)}\right) \tag{7}$$

depends only on the transmit-power of SU m and the scheduling variable $w_{m,n}$. Let $i^{\max} \in (0,1)$ denote the maximum long-term probability (rate) of interference. Then, the following constraint must hold

$$\mathbb{E}_{\mathbf{g},\mathbf{s}}\left[\sum_{(m,n)\in\mathcal{E}} w_{m,n}(\mathbf{g},\mathbf{s})i_{m,n}(p_{m,n}(\mathbf{g},\mathbf{s}),\mathbf{s})\right] \leq i^{\max}. \tag{8}$$

SU-to-SU channels $\mathbf{g}$ vary across time due to fading. Thus, the SU network operates in a time-slotted setup, where the duration of each slot (indexed by t) corresponds to the coherence time of the small-scale fading process. The PSI $\mathbf{s}$ may also vary (due to, e.g., PU mobility), but at a larger time scale. Thus, since $\{r_{n,m}^k, w_{m,n}, p_{m,n}\}$ are computed based on $\mathbf{g},\mathbf{s}$, it follows that $\{r_{n,m}^k, w_{m,n}, p_{m,n}\}$ vary with time too. Henceforth, $\mathbf{g}$, $\mathbf{s}$, $r_{n,m}^k(\mathbf{g},\mathbf{s})$, $w_{m,n}(\mathbf{g},\mathbf{s})$, and $p_{m,n}(\mathbf{g},\mathbf{s})$ will be replaced by $\mathbf{g}[t]$, $\mathbf{s}[t]$, $r_{n,m}^k[t]$, $w_{m,n}[t]$, and $p_{m,n}[t]$ whenever time dependence is to be stressed. The metric to be optimized will be designed to discourage high average power consumptions, while promoting high exogenous traffic rates. To this end, let $V_m^k(a_m^k)$ denote a concave, non-decreasing, utility function quantifying the reward associated with the

exogenous rate a_m^k, and $J_m(\bar{p}_m)$ be a convex, non-decreasing, function representing the cost incurred by U_m when its average transmit-power is $\bar{p}_m$ [19]. The metric to be maximized is then

$$f(\{a_m^k\},\{\bar{p}_m\}) := \sum_{m,k} V_m^k(a_m^k) - \sum_m J_m(\bar{p}_m)\,. \quad (9)$$

Based on the preceding discussion and with $\mathcal{Y} := \{a_m^k, \bar{p}_m, r_{n,m}^k(\mathbf{g},\mathbf{s}), w_{m,n}(\mathbf{g},\mathbf{s}), p_{m,n}(\mathbf{g},\mathbf{s}), \forall m,n \in \mathcal{N}_m, \mathbf{g},\mathbf{s}\}$ collecting all the design variables, the optimal cross-layer RA for the SU network subject to ("s. to") interference constraints is designed as the solution of

$$\mathsf{P}^* := \max_{\mathcal{Y}} \sum_{m,k} V_m^k(a_m^k) - \sum_m J_m(\bar{p}_m) \quad (10a)$$

$$\text{s.to}: (1),\ (2),\ (8),\ \text{and} \quad (10b)$$

$$\sum_k r_{m,n}^k(\mathbf{g},\mathbf{s}) \le w_{m,n}(\mathbf{g},\mathbf{s}) C_{m,n}(\mathbf{g}, p_{m,n}(\mathbf{g},\mathbf{s})) \quad (10c)$$

$$\mathbb{E}_{\mathbf{g},\mathbf{s}}\left[\sum_{n\in\mathcal{N}_m} w_{m,n}(\mathbf{g},\mathbf{s}) p_{m,n}(\mathbf{g},\mathbf{s})\right] \le \bar{p}_m \quad (10d)$$

$$w_{m,n}(\mathbf{g},\mathbf{s}) \in \{0,1\},\ a_m^{k,\min} \le a_m^k \le a_m^{k,\max}\ \ 0 \le r_{m,n}^k \quad (10e)$$

$$0 \le p_{m,n} \le p_m^{\max},\ 0 \le \bar{p}_{m,n} \le \bar{p}_m^{\max} \quad (10f)$$

where $a_m^{k,\min}$ and $a_m^{k,\max}$ are arrival rate requirements; (10d) has been relaxed and written as an inequality [cf. (3)] without loss of optimality; and (10c) dictates that the rate at the network level cannot exceed the one at the link layer. If needed, (10c) can be modified to account for losses due to packet/frame headers.

Unfortunately, (10) is a challenging non-convex problem. Specifically, nonconvexity emerges because:
i) $\{w_{m,n}(\mathbf{g},\mathbf{s})\}$ are binary variables;
ii) the monomials $w_{m,n}(\mathbf{g},\mathbf{s})p_{m,n}(\mathbf{g},\mathbf{s})$ and $w_{m,n}(\mathbf{g},\mathbf{s})C_{m,n}(p_{m,n}(\mathbf{g},\mathbf{s}))$ are not *jointly* convex in $w_{m,n}$ and $p_{m,n}$; and,
iii) the interference constraint (8) is nonconvex. Despite these difficulties, it will be shown in the ensuing section that the *optimal* solution can be obtained.

III. Optimal Adaptive RA

Consider first relaxing the binary scheduling constraints $w_{m,n}(\mathbf{g},\mathbf{s}) \in \{0,1\}$ as $w_{m,n}(\mathbf{g},\mathbf{s}) \in [0,1]$. Since constraints (2), (10c), (10d), and (8) are linear w.r.t. $w_{m,n}(\mathbf{g},\mathbf{s})$, each of the optimal arguments $\{w_{m,n}^*\}$ of the resultant relaxed problem lies at one of the boundaries of interval $[0,1]$; thus, $\{w_{m,n}^*\}$ in the relaxed problem coincide with the ones of (10). See the Appendix for a formal discussion. Next, to cope with the nonconvexity of the monomial $w_{m,n}(\mathbf{g},\mathbf{s})p_{m,n}(\mathbf{g},\mathbf{s})$ and function $w_{m,n}(\mathbf{g},\mathbf{s})C_{m,n}(\mathbf{g}, p_{m,n}(\mathbf{g},\mathbf{s}))$, consider introducing the auxiliary variables $\tilde{p}_{m,n}(\mathbf{g},\mathbf{s}) := w_{m,n}(\mathbf{g},\mathbf{s})p_{m,n}(\mathbf{g},\mathbf{s})$, $(m,n) \in \mathcal{E}$. It can be readily verified that the Hessian of the function $w_{m,n}(\mathbf{g},\mathbf{s})C_{m,n}(\mathbf{g},\tilde{p}_{m,n}(\mathbf{g},\mathbf{s})/w_{m,n}(\mathbf{g},\mathbf{s}))$ is seminegative definite, and thus the surrogate of (10c) is convex. Unfortunately, there is no immediate way to address the nonconvexity of (8). Nevertheless, one can leverage the results of [25, Thm. 1] to show that the duality gap is *zero*, and adopt a Lagrangian dual approach *without* loss of optimality. What is more, it will be shown that the minimization of the Lagrangian can be carried out in a computationally-efficient manner, thank to a favorable structure of the Lagrangian.

To this end, consider dualizing the average constraints, and let $\{\lambda_m^k\}$, θ, and $\{\pi_m\}$ denote the multipliers associated with (1), (8), and (10d), respectively. Thus, with $\mathbf{d} := \{\lambda_m^k, \pi_m, \theta\}$, the (partial) Lagrangian of (10) amounts to

$$\begin{aligned}\mathcal{L}(\mathcal{Y},\mathbf{d}) :=& \sum_{m,k} V_m^k(a_m^k) - \sum_m J_m(\bar{p}_m)\\ &- \sum_{m,k}\lambda_m^k\left(a_m^k + \sum_{n\in\mathcal{N}_m}\left(\mathbb{E}_{\mathbf{g},\mathbf{s}}\left[r_{n,m}^k(\mathbf{g},\mathbf{s}) - r_{m,n}^k(\mathbf{g},\mathbf{s})\right]\right)\right)\\ &- \theta\left(\mathbb{E}_{\mathbf{g},\mathbf{s}}\left[\sum_{(m,n)\in\mathcal{E}} w_{m,n}(\mathbf{g},\mathbf{s}) i_{m,n}(\tilde{p}_{m,n},\mathbf{s})\right] - i^{\max}\right)\\ &- \sum_m \pi_m\left(\mathbb{E}_{\mathbf{g},\mathbf{s}}\left[\sum_{n\in\mathcal{N}_m}\tilde{p}_{m,n}(\mathbf{g},\mathbf{s})\right] - \bar{p}_m\right). \quad (11)\end{aligned}$$

Assuming that the optimal multipliers $\{\lambda_m^{k*}, \pi_m^*, \theta^*\}$ are available, the optimal primal variables can be computed as follows.

Proposition 1. *The optimal average transmit-power $\bar{p}_m^*$ of node U_m is found as the solution of the scalar convex program*

$$\bar{p}_m^*(\pi_m^*) := \underset{0\le\bar{p}_m\le\bar{p}_m^{\max}}{\arg\max} \ -J_m(\bar{p}_m) + \pi_m^*\bar{p}_m\,. \quad (12)$$

If $\dot{J}_m(\pi_m)$ exists and is invertible, it follows that

$$\bar{p}_m(\pi_m^*) = \left[(\dot{J}_m)^{-1}(\pi_m^*)\right]_0^{\bar{p}_m^{\max}}. \quad (13)$$

This result can be obtained by isolating the terms in $\mathcal{L}(\mathcal{Y},\mathbf{d}^*)$ that depend on $\{\bar{p}_m\}$, maximizing those terms separately, and subsequently projecting the solution onto the feasible set $[0,\bar{p}_m^{\max}]$. Following similar steps, the optimal average exogenous rates can be found as specified next.

Proposition 2. *Given the optimal dual variables $\{\lambda_m^{k*}\}$, the optimal exogenous rates $\{a_m^{k*}\}$ are*

$$a_m^{k*}(\lambda_m^{k*}) = \underset{a_m^{k,\min}\le a\le a_m^{k,\max}}{\arg\max} \ V_m^k(a) - \lambda_m^{k*}a\,. \quad (14)$$

When the inverse of $\dot{V}_m^k(a)$ exists, a_m^{k*} can be obtained in closed form as

$$a_m^{k*}(\lambda_m^{k*}) = \left[(\dot{V}_m^k)^{-1}(\lambda_m^{k*})\right]_{a_m^{k,\min}}^{a_m^{k,\max}}. \quad (15)$$

As expected, the optimal flow policy (14) takes into account both the reward $V_m^k(a_m^k)$, and the "price" λ_m^{k*} for injecting exogenous traffic at a rate a_m^k into the network. Similarly, the optimal average power in (12) is set by balancing the cost $J_m(\bar{p}_m)$ with the reward represented by π_m^*.

Towards finding the optimal routing, scheduling, and instantaneous transmit-powers, define for each link (m,n) the coefficients

$$\lambda_{m,n}^{k*} := \lambda_m^{k*} - \lambda_n^{k*} \ \text{ and } \ \lambda_{m,n}^* := \max_k\{\lambda_{m,n}^{k*}\} \quad (16)$$

along with the functional

$$\varphi_{m,n}(\mathbf{g}[t],p,\mathbf{d}^*) := \Big[\lambda^*_{m,n}C_{m,n}(\mathbf{g}[t],p) - \pi^*_m p - \theta^*\mathbb{E}_{\mathbf{s}[t]}\left[i_{m,n}(p,\mathbf{s}[t])\right]\Big]_+ \quad (17)$$

where $\{\mathbf{g}[t],\mathbf{s}[t]\}$ are the realizations of $\{\mathbf{g},\mathbf{s}\}$ at slot t. Under *(as1)–(as2)*, the expected value $\mathbb{E}_{\mathbf{s}[t]}\left[i_{m,n}(p,\mathbf{s}[t])\right]$ can be written as

$$\mathbb{E}_{\mathbf{s}[t]}\left[i_{m,n}(p,\mathbf{s}[t])\right] = 1 - \prod_{q=1}^{Q}\Big(1 - \sum_{\mathbf{x}\in\mathcal{G}} \iota_{m,\mathbf{x}^{(q)}}(p,\mathbf{s}[t])\beta^{(q)}_{\mathbf{x}}\Big) \quad (18)$$

with $\iota_{m,\mathbf{x}^{(q)}}(p,\mathbf{s}[t]) := \Pr\left\{p\,h_{m,\mathbf{x}^{(q)}} > I\right\}$. The previous probability can be either evaluated numerically or, for tractable fading distributions, computed in closed form. For example, if $h_{m,\mathbf{x}}$ is Rayleigh distributed, then $\iota_{m,\mathbf{x}}(p,\mathbf{s}[t]) = e^{-I/(p\gamma_{m,\mathbf{x}}[t])}$ with $\gamma_{m,\mathbf{x}}$ denoting the path loss between SU U_m and grid point $\mathbf{x}$ [20].

Using (16) and (17), optimal rates $\{r^{k*}_{m,n}[t]\}$, scheduling variables $\{w^*_{m,n}[t]\}$, and instantaneous transmit-powers $\{p^*_{m,n}[t]\}$ are found as specified next (the proofs are outlined in the Appendix).

Proposition 3. *Given* $\mathbf{g}[t]$ *and* $\mathbf{s}[t]$*, the optimal* $\{p^*_{m,n}[t], w^*_{m,n}[t]\}$ *are*

$$p^*_{m,n}[t] := \left[\arg\max_p\ \varphi_m(\mathbf{g}[t],p,\mathbf{d}^*))\right]_0^{p^{\max}_m} \quad (19)$$

$$w^*_{m,n}[t] := \mathbb{1}_{\{(m,n)=\arg\max_{(i,j)\in\mathcal{E}}\varphi_{m,n}(\mathbf{g}[t],p^*_{m,n}[t],\mathbf{d}^*)\}}. \quad (20)$$

Proposition 4. *Per link* $(m,n)\in\mathcal{E}$*, define the set* $\mathcal{K}_{m,n}[t] := \{k : k = \arg\max_j\{\lambda^j_{m,n}\} \wedge \lambda^{k*}_{m,n} \geq 0\}$*. Then, the optimal* $\{r^{k*}_{m,n}[t]\}$ *satisfy the following two conditions:*
r1) if $k\notin\mathcal{K}_{m,n}[t]$*, then* $r^{k*}_{m,n}[t]=0$*; and,*
r2) if $|\mathcal{K}_{m,n}[t]|\geq 1$*, if follows that* $\sum_{k\in\mathcal{K}_{m,n}[t]} r^{k*}_{m,n}[t] = w^*_{m,n}[t]\,C_{m,n}(\mathbf{g}[t],p^*_{m,n}[t])$.

Clearly, when $|\mathcal{K}_{m,n}[t]|=1$*, one has the "winner-takes-all" solution*

$$r^{k*}_{m,n}[t] = \mathbb{1}_{\{k\in\mathcal{K}_{m,n}[t]\}} w^*_{m,n}[t]\,C_{m,n}(\mathbf{g}[t],p^*_{m,n}[t]). \quad (21)$$

Key to understanding the solution of Proposition 3 is the definition of $\varphi_{m,n}(\mathbf{g}[t],p,\mathbf{d}^*)$. Intuitively, (17) can be interpreted as an instantaneous link-quality indicator, which dictates a trade-off between the instantaneous transmit-rate, transmit-power and interference (with the multipliers $\lambda^*_{m,n}$, π^*_m and θ^* representing the prices of the corresponding resources). Interestingly, (19) reveals that $p^*_{m,n}[t]$ is found by maximizing $\varphi_{m,n}(\mathbf{g}[t],p,\mathbf{d}^*)$, which does not depend on information of links other than $U_m\to U_n$. In other words, the optimization problem in the dual domain is separable across SU links (and time). For many fading distributions, (19) turns out to be nonconvex. However, since only one scalar variable is involved, the optimal transmit-power $p^*_{m,n}[t]$ can be found efficiently. Proposition 4 describes the operation of the routing protocol and establishes that only flows with the highest value of $\lambda^{k*}_{m,n}$ can be routed. Clearly, the multiplier λ^{k*}_m can be viewed as a congestion indicator of flow k at node m, so that the optimum solution dictates that flows have to follow routes that maximize the difference $\lambda^{k*}_{m,n} = \lambda^{k*}_n - \lambda^{k*}_m$. This reveals that the solution reduces the network congestion (in fact, links to the well-known *back-pressure* routing algorithm can be established [19]). Further, it worth stressing that the value of the channel gain of a SU-to-SU link does not affect how different flows share that link, but only the number of packets routed through it; i.e., only $C_{m,n}(\mathbf{g}[t],p^*_{m,n}[t])$.

The next subsection deals with the estimation of the optimum Lagrange multipliers. But first, a remark is in order.

Remark 1 (Contention graph). In lieu of (2), the notion of "contention graph" is oftentimes advocated in conventional multi-hop wireless setups to possibly activate multiple wireless links simultaneously; see e.g., [26], [27]. Taking a similar approach for the problem at hand is challenging because: *i)* presence of the probability-of-interference constraints would render the definition of such a graph non-trivial; and, *ii)* the power optimization would be coupled across SUs. Development of *approximate* solutions tailored to the problem at hand are left as future work.

A. Estimating the optimum Lagrange multipliers

Finding the optimal dual variables $\{\lambda^{k*}_m,\pi^*_m,\theta^*\}$ may be computational challenging because: *a)* classical iterative subgradient methods require, at each iteration, averaging over all $\mathbf{g}$ and $\mathbf{s}$ realizations; and, *b)* if either the channel statistics or the number of users change, $\{\lambda^{k*}_m,\pi^*_m,\theta^*\}$ must be recomputed. An effective alternative consists in resorting to stochastic approximation iterations [28], [29], whose goal is to obtain samples $\{\lambda^k_m[t],\pi_m[t],\theta[t]\}$, $t=1,2,\ldots$ that are nevertheless sufficiently close to the optimal dual variables.

The merit of stochastic approximation techniques is twofold: *i)* computational complexity of the stochastic approximation schemes is markedly lower than that of their off-line counterparts; and, *ii)* stochastic schemes can cope with non-stationary propagation channels and dynamic PU activities. With $\mu_\lambda>0$, $\mu_\pi>0$, and $\mu_\theta>0$ denoting constant stepsizes, the following stochastic iterations yield the desired multipliers $\forall\, t$:

$$\lambda^k_m[t+1] = \Big[\lambda^k_m[t] + \mu_\lambda\Big(a^{k*}_m(\lambda^k_m[t]) + \sum_{n\in\mathcal{N}_m}(r^{k*}_{n,m}[t] - r^{k*}_{m,n})[t]\Big)\Big]_+ \quad (22)$$

$$\pi_m[t+1] = \Big[\pi_m[t] - \mu_\pi\Big(\bar{p}^*_m(\pi_m[t]) - \sum_{n\in\mathcal{N}_m} w^*_{m,n}[t]p^*_{m,n}[t]\Big)\Big]_+ \quad (23)$$

$$\theta[t+1] = \Big[\theta[t] - \mu_\theta\Big(i^{\max} - i(\{p^*_{m,n}[t]\},\mathbf{s}[t])\Big)\Big]_+. \quad (24)$$

The update terms in the right hand side of (22)-(24) form an *unbiased* stochastic subgradient of the dual function of (10), and they are *bounded*; see, e.g., [30]. Using these two features, the following convergence and feasibility result can be established.

Proposition 5. *Define* $\mu := \max\{\mu_\lambda,\mu_\pi,\mu_\theta\}$*;* $\bar{P}[t] := \frac{1}{t}\sum_{\tau=1}^t\sum_m J_m(p^*_m[\tau]) - \sum_{m,k}V^k_m(a^{k*}_m(\lambda^k_m[\tau]))$*; and,* $\bar{i}[t] := \frac{1}{t}\sum_{\tau=1}^t i(\{p_{m,n}[\tau]\},\mathbf{s}[\tau])$*. Then, it holds with probability one that as* $t\to\infty$ *the sample average of the*

stochastic RA:
i) *is feasible and, thus,* $\bar{i}[t] \leq i^{max}$*; and,*
ii) *incurs minimal performance loss w.r.t. the optimal solution of* (10)*; i.e,* $\bar{P}[t] \geq P^* - \delta(\mu)$*, where* $\delta(\mu) \to 0$ *as* $\mu \to 0$*.*

A proof of this result is not presented here due to space limitations, but it relies on the convergence of stochastic (epsilon) subgradient methods and can be obtained following the lines of [19], [29]. The key to prove *i)* is to show that the stochastic multipliers are bounded. This can be readily used to show the asymptotic feasibility of the sample averages of the stochastic subgradients, i.e., of the update terms in (22)-(24). The proof for *ii)* is a bit more intricate and leverages properties of the dual function, the convexity of the objective function in (10a), and the bounds on the stochastic updates. It turns out that the loss of optimality $\delta(\mu)$ is linear w.r.t. both μ and G, which represents an upperbound on the expected squared norm of the stochastic subgradient. Clearly, this implies that $\delta(\mu) \to 0$ as $\mu \to 0$.

B. Individual interference constraints

The developed RA scheme controls the interference inflicted to the primary *system*. However, it may turn that some PUs are interfered more frequently than others. To eliminate this discrepancy, probability-of-interference constraints can be placed on a per-PU receiver basis. The changes required in the optimal RA schemes to address this case are oulined next.

Define as $i^{(q)}_{m,n}(p,\mathbf{s}) := \sum_{\mathbf{x}\in\mathcal{G}} z^{(q)}_{\mathbf{x}} \mathbb{1}_{\{ph_{m,\mathbf{x}^{(q)}}>I\}}$ [cf. (7)] the probability of interfering with the PU receiver q when link $U_m \to U_n$ is scheduled. Then, the individual probability-of-interference constraints amount to [cf. (8)]

$$\mathbb{E}_{\mathbf{g},\mathbf{s}}\left[\sum_{(m,n)\in\mathcal{E}} w_{m,n}(\mathbf{g},\mathbf{s}) i^{(q)}_{m,n}(p_{m,n}(\mathbf{g},\mathbf{s}),\mathbf{s})\right] \leq i^{q,\max} \quad (25)$$

where $i^{q,\max}$ can either be set to the same value for all q, or, be customized. The next step is to modify the optimization problem (10) by replacing the single constraint (8) with the Q constraints (one per user) in (25). Each of the new constraints is dualized (with θ^q denoting the corresponding multiplier) and incorporated into the Lagrangian in (11). The only change required in the expressions for the optimal RA is re-definition of the link-quality indicator in (17) as $\varphi_{m,n}(\mathbf{g}[t],p,\mathbf{d}^*) := [\lambda^*_{m,n} C_{m,n}(\mathbf{g}[t],p) - \pi^*_m p - \sum_q \theta^{q*} \mathbb{E}_{\mathbf{s}[t]}[i^{(q)}_{m,n}(p,\mathbf{s}[t])]]_+$. All other expressions for the optimal RA (including results in Propositions 1-4) remain the same.

The last step is to modify the stochastic update for the multiplier in (24). Instead of the single update for $\theta[t+1]$, the following Q updates are needed $\theta^q[t+1] = [\theta^q[t] - \mu_\theta(i^{\max}_{(q)} - i^{(q)}[t])]_+$, where $i^{(q)}[t] = 1$ if the PU receiver q has been interfered. Such an information is either broadcasted by the PU system or estimated from the available observations (see next section for details). If all constraints are active, then all the multipliers will be non-zero. However, there are scenarios where that would not be the case, e.g., if a PU receiver is very far away. In those cases, the stochastic estimate of the corresponding multiplier remains zero most of the time.

IV. Receiver-map estimation

The SU network relies on perfect CSI $\mathbf{g}$, probabilities $\{\iota_{m,n,\mathbf{x}}\}$ and the PU receivers' spatial distribution $\{\beta^{(q)}_{\mathbf{x}}\}$ to schedule SU transmissions, while adhering to the long-term interference constraints [cf. (17)]. The SU-to-SU gains $\mathbf{g}$ are acquired via conventional sensing. Moreover, once the virtual grid $\mathcal{G}$ is chosen, $\{\iota_{m,n,\mathbf{x}}\}$ can be computed as a function of the transmit-powers $\{p_{m,n}\}$. The aim here is to develop an online Bayesian estimator for $\{\beta^{(q)}_{\mathbf{x}}\}$, based on a minimal interplay between PU and SU systems. Specifically, the following setup is considered.

(as3) The PU system notifies the secondary network if disruptive interference occurrs to one or more PU receivers.

Two interference announcement strategies are considered:

(c1) the PU system broadcasts the message $i^{(q)}[t] = 1$ to notify that the event $p^*_{m^*,n^*} h_{m^*,\mathbf{x}^{(q)}} > I$ occurred; and,
(c2) the generic message $i[t] = 1$ is transmitted if at least one of the PU receivers were disruptively interfered.

In both setups, just *one*-bit is sufficient to notify the SU system that the instantaneous interference inflicted to one or more PU receivers exceeds the tolerable level I. In *(c2)*, this interference tweet is sent by, e.g., a base station or a primary NC. In this message, no information regarding the PU user(s) interfered is provided. As for *(c1)*, the interference tweet can be sent by either the primary NC (requiring additional few bits to indicate the PU interfered), or, by the interfered PU receivers themselves (with the PU identifier included as usual in the packet header).

Similar modeling assumptions were made in, e.g., [5] and [18] (see also references therein), where the PU's Automatic Repeat-reQuests (ARQs) are assumed to be either exchanged or eavesdropped by the SU transceivers. With the overheard ARQs, the SUs can evaluate the outage rates of ongoing PU communications, and adjust their transmit-powers accordingly [5]. In lieu of outage rates, PU receiver locations may be estimated. However, localization based on RSS measurements over a single ARQ packet is challenging because of, e.g., PU mobility and fast time-varying fading. A more conservative (but suboptimal) approach that bypasses the need to know PU receiver locations is to guarantee that the interference does not exceed a prescribed level at any boundary point of the PU transmitters' coverage region [10], [13], [14], which can be estimated during the sensing phase [11], [13]. This amounts to arranging $Q = |\mathcal{G}|$ grid points in the boundary of the coverage region, and setting $\beta^{(q)}_{\mathbf{x}} = 1$ for all $q = 1,\ldots,Q$.

A. Per-PU receiver notification

To account for PU mobility, we assume that:
(as4) $z^{(p)}_{\mathbf{x}}[t]$ is a first-order (spatiotemporal) Markov process with *known* transition probabilities $\phi^{(q)}_{\mathbf{x},\mathbf{x}'}[t] := \Pr\{z^{f,(q)}_{\mathbf{x}}[t] = 1 | z^{(q)}_{\mathbf{x}'}[t-1] = 1\}$.

To decrease the computational burden, $\phi^{(q)}_{\mathbf{x},\mathbf{x}'}[t]$ are further assumed to be nonzero only if $\mathbf{x}' \in \mathcal{G}_{\mathbf{x}}$, where the set $\mathcal{G}_{\mathbf{x}}$ contains $\mathbf{x}$ and its neighboring grid points. Collect in the

set $\mathcal{I}_t^{(q)} := \{i^{(q)}[\tau]\}_{\tau=1}^t$ the interference notifications up to time slot t, and define further the sets $\tilde{\mathcal{H}}_t^{(q)} := \mathcal{I}_{t-1}^{(q)} \cup \{p_{m,n}^*[t], w_{m,n}^*[t],\ \forall(m,n)\}_{\tau=1}^t$ and $\mathcal{H}_t^{(q)} := \tilde{\mathcal{H}}_t^{(q)} \cup i^{(q)}[t]$. Since the elements of $\mathcal{I}_t^{(q)}$ constitute the observed states of a Hidden Markov Model (HMM), a recursive Bayesian estimator can be implemented to acquire (and track) the posterior probability mass function of $\{z_{\mathbf{x}}^{(q)}\}_{\mathbf{x}\in\mathcal{G}}$. To this end, let $\hat{\beta}_{\mathbf{x}}^{(q)}[t|t-1] := \Pr\{z_{\mathbf{x}}^{(q)}[t] = 1|\mathcal{H}_{t-1}^{(q)}\}$ and $\hat{\beta}_{\mathbf{x}}^{(q)}[t|t] := \Pr\{z_{\mathbf{x}}^{(q)}[t] = 1|\mathcal{H}_t^{(q)}\}$ denote the instantaneous beliefs given $\mathcal{H}_{t-1}^{(q)}$ and $\mathcal{H}_t^{(q)}$, respectively. Finally, let $(m^*, n^*) := \arg\max_{(i,j)\in\mathcal{E}} w_{m,n}^*[t]$ denote the scheduled link at time t. Thus, the receiver maps can be recursively updated by performing the following steps per grid point $\mathbf{x}$ and PU receiver q (see, e.g., [15]).

Prediction step:

$$\hat{\beta}_{\mathbf{x}}^{(q)}[t|t-1] = \sum_{\mathbf{x}'\in\mathcal{G}_{\mathbf{x}}} \phi_{\mathbf{x},\mathbf{x}'}^{(q)}[t]\hat{\beta}_{\mathbf{x}}^{(q)}[t-1|t-1]\,. \tag{26}$$

Correction step:

$$\hat{\beta}_{\mathbf{x}}^{(q)}[t|t] = \frac{\Pr\{i^{(q)}[t] = o|z_{\mathbf{x}}^{(q)}[t] = 1, \tilde{\mathcal{H}}_t^{(q)}\}\hat{\beta}_{\mathbf{x}}^{(q)}[t|t-1]}{\Pr\{i^{(q)}[t] = o|\tilde{\mathcal{H}}_t^{(q)}\}} \tag{27}$$

where $o \in \{0,1\}$ denotes the value observed for $i^{(q)}[t]$.

Suppose that $i^{(q)}[t] = 1$. Then, noticing that $z_{\mathbf{x}}^{(q)}[t] = 1$ implies that $z_{\mathbf{x}'}^{(q)}[t] = 0$ for the grid points $\mathbf{x}' \in \mathcal{G}\backslash\{\mathbf{x}\}$, it follows that $\Pr\{i^{(q)}[t] = 1|z_{\mathbf{x}}^{(q)}[t] = 1, \tilde{\mathcal{H}}_t^{(q)}\} = \iota_{m,\mathbf{x}}(p_{m^*,n^*}^*, \mathbf{s}[t])$. As for the denominator in (27), one only has to average the numerator over all possible locations. For $i^{(q)}[t] = 1$ this entails

$$\begin{aligned}
&\Pr\{i^{(q)}[t] = 1|\tilde{\mathcal{H}}_t^{(q)}\} \\
&= \sum_{\mathbf{x}'\in\mathcal{G}} \Pr\left\{i^{(q)}[t] = 1|z_{\mathbf{x}'}^{(q)}[t] = 1, \tilde{\mathcal{H}}_t^{(q)}\right\} \hat{\beta}_{\mathbf{x}'}^{(q)}[t|t-1] && \text{(28a)}\\
&= \sum_{\mathbf{x}'\in\mathcal{G}} \iota_{m,\mathbf{x}'}(p_{m^*,n^*}^*, \mathbf{s}[t])\hat{\beta}_{\mathbf{x}'}^{(q)}[t|t-1]. && \text{(28b)}
\end{aligned}$$

Thus, when interference is inflicted to the PU receiver q, (27) can be simplified to:

$$\hat{\beta}_{\mathbf{x}}^{(q)}[t|t] = \frac{\iota_{m,\mathbf{x}}(p_{m^*,n^*}^*, \mathbf{s}[t])\hat{\beta}_{\mathbf{x}}^{(q)}[t|t-1]}{\sum_{\mathbf{x}'\in\mathcal{G}_{\mathbf{x}}} \iota_{m,\mathbf{x}'}(p_{m^*,n^*}^*, \mathbf{s}[t])\,\hat{\beta}_{\mathbf{x}'}^{(q)}[t|t-1]} \tag{29}$$

and can be readily computed once the SU-to-grid point channel distribution is known. The counterpart of (37) for $i^{(q)}[t] = 0$ is computed in the obvious way.

In this setup, the secondary system *does not* require prior knowledge of Q. Rather, the set $\mathcal{Q}$ of PU receivers that can be potentially interfered is updated on-line based on the messages $\{i^{(q)}[\tau] = 1\}$. For example, $\mathcal{Q}[t] = \mathcal{Q}[t-1] \cup \{q\}$ whenever $i^{(q)}[t] = 1$ and $q \neq \mathcal{Q}[t-1]$. On the other hand, $\mathcal{Q}[t]$ is updated as $\mathcal{Q}[t] = \mathcal{Q}[t-1]\backslash\{q\}$ when no messages are received from PU q for a prolonged period of time.

B. System-wide interference announcement

Similar to Section IV-A, let $\mathcal{I}_t := \{i[\tau]\}_{\tau=1}^t$ denote the set collecting the interference notifications, and let $\tilde{\mathcal{H}}_t := \mathcal{I}_{t-1} \cup \{p_{m,n}^*[\tau], w_{m,n}^*[\tau],\ \forall(m,n)\}_{\tau=1}^t$ and $\mathcal{H}_t := \tilde{\mathcal{H}}_t \cup i[t]$. Further, re-define the instantaneous beliefs $\hat{\beta}_{\mathbf{x}}^{(q)}[t|t-1]$ and $\hat{\beta}_{\mathbf{x}}^{(q)}[t|t-1]$ as $\beta_{\mathbf{x}}^{(q)}[t|t-1] := \Pr\{z_{\mathbf{x}}^{(q)}[t] = 1|\mathcal{H}_{t-1}\}$ and $\beta_{\mathbf{x}}^{(q)}[t|t] := \Pr\{z_{\mathbf{x}}^{(q)}[t] = 1|\mathcal{H}_t\}$, respectively. With $\mathcal{I}_t$ representing again the observed states of an HMM, the prediction step of the resultant recursive Bayesian estimator is computed as in (26). On the other hand, the correction step becomes in this case

$$\hat{\beta}_{\mathbf{x}}^{(q)}[t|t] = \frac{\Pr\{i[t] = o|z_{\mathbf{x}}^{(q)}[t] = 1, \tilde{\mathcal{H}}_t\}\hat{\beta}_{\mathbf{x}}^{(q)}[t|t-1]}{\Pr\{i[t] = o|\tilde{\mathcal{H}}_t\}} \tag{30}$$

where $o \in \{0,1\}$ denotes the value observed for $i[t]$.

To further elaborate on (30), the following modeling assumption is made.

(as5) The value (or an upper bound) of Q is known.

Section V will illustrate that *(as5)* is not very restrictive, since just an upperbound on the number of PU receivers Q suffices to carry out the localization task. More sophisticated schemes that jointly estimate and track Q and $\{\beta_{\mathbf{x}}^{(q)}\}$ are of interest, but they will be the subject of future research. When $i[t] = 0$, the denominator of (30) is given by

$$\begin{aligned}
&\Pr\{i[t] = 0|\tilde{\mathcal{H}}_t\} \\
&= \Pr\{i^{(1)}[t] = 0, \ldots, i^{(Q)}[t] = 0|\tilde{\mathcal{H}}_t\} && \text{(31a)}\\
&= \prod_{q=1}^{Q} \left(1 - \Pr\{i^{(q)}[t] = 1|\tilde{\mathcal{H}}_t\}\right) && \text{(31b)}\\
&= \prod_{q=1}^{Q} \left(1 - \sum_{\mathbf{x}\in\mathcal{G}} \iota_{m,\mathbf{x}}(p_{m^*,n^*}^*[t], \mathbf{s}[t])\hat{\beta}_{\mathbf{x}}^{(q)}[t|t-1]\right) && \text{(31c)}
\end{aligned}$$

where (31b) follows (31a) because of *(as1)* and *(as2)*. The latter assumption holds also when two (or more) PU receivers reside in proximity of the same grid point, provided they are a few wavelengths apart [20, Ch. 3]. Clearly, for $i[t] = 1$, $\Pr\{i[t] = 1|\tilde{\mathcal{H}}_t\}$ is readily obtained as $\Pr\{i[t] = 1|\tilde{\mathcal{H}}_t\} = 1 - \Pr\{i[t] = 0|\tilde{\mathcal{H}}_t\}$. Using similar steps, one can show that $\Pr\{i[t] = 0|z_{\mathbf{x}}^{(q)}[t] = 1, \tilde{\mathcal{H}}_t\}$ can be re-expressed as

$$\begin{aligned}
&\Pr\{i[t] = 0|z_{\mathbf{x}}^{(q)}[t] = 1, \tilde{\mathcal{H}}_t\} \\
&= \Pr\{i^{(1)}[t] = 0, \ldots, i^{(Q)}[t] = 0|z_{\mathbf{x}}^{(q)}[t] = 1, \tilde{\mathcal{H}}_t\} && \text{(32a)}\\
&= \Pr\{i^{(q)}[t] = 0|z_{\mathbf{x}}^{(q)}[t] = 1, \tilde{\mathcal{H}}_t\} \\
&\times \prod_{u=1,u\neq q}^{Q} \left(1 - \sum_{\mathbf{x}'\in\mathcal{G}} \iota_{m,\mathbf{x}'}(p_{m^*,n^*}^*[t], \mathbf{s}[t])\hat{\beta}_{\mathbf{x}'}^{(u)}[t|t-1]\right) && \text{(32b)}
\end{aligned}$$

where $\Pr\{i^{(q)}[t] = 0|z_{\mathbf{x}}^{(q)}[t] = 1, \tilde{\mathcal{H}}_t\}$ can be further expressed as $\Pr\{i^{(q)}[t] = 0|z_{\mathbf{x}}^{(q)}[t] = 1, \tilde{\mathcal{H}}_t\} = 1 - \iota_{m,\mathbf{x}}(p_{m^*,n^*}^*, \mathbf{s}[t])$.

C. Receiver-map-cognizant RA

The receiver maps are used to evaluate the interference term in functional $\varphi_{m,n}$ [cf. (18)], which clearly affects the computation of the optimal transmit-powers $p_{m,n}^*[t]$ and scheduling variables $w_{m,n}^*[t]$ [cf. (19)-(20)]. Equation (18) implies that if the location of the PU receivers is perfectly known, only their corresponding terms $\{\mathbf{x}^{(q)}\}_{q=1}^Q$ will enter in the summation. On the other hand, if the actual location is uncertain, the interference generated at each point of the grid

Algorithm 1 Joint RA and receiver-map estimation

Initialize $\mathcal{Y}[0]$, $\mathbf{d}[0]$, and $\{\hat{\beta}_{\mathbf{x}}^{(q)}[0|0]\}$.
for $t = 1, \ldots$ (repeat until convergence) **do**
[s1] Perform the prediction step (26).
[s2] Acquire SU-to-SU channels $\{g_{m,n}[t]\}$.
[s3] Obtain $\{a_m^{k*}(\mathbf{d}[t-1])\}, \{r_{m,n}^{k*}[t-1]\}, \{\bar{p}_m^*(\mathbf{d}[t-1])\}$ via (15), (21), and (12)
[s4] Obtain $\{w_{m,n}^*[t], p_{m,n}^*[t]\}$ via (19)–(20), where $\{\beta_{\mathbf{x}}^{(q)}\}$ in (18) is replaced by $\{\hat{\beta}_{\mathbf{x}}^{(q)}[t|t-1]\}$.
[s5] Update $\{\lambda_m^k[t]\}, \{\pi_m[t]\}$ via (22)–(23).
[s5] Receive $i^{(q)}[t]$ (or $i[t]$), if interference occurred.
[s6] Update $\theta[t]$ via (24), using the observed $i^{(q)}[t]$ (or $i[t]$).
[s7] Run the correction step (27) (or (30)).
end for

will be weighted by the probability of the PU receiver residing there. Hence, at slot t, the beliefs $\{\hat{\beta}_{\mathbf{x}}^{(q)}[t|t-1]\}$ are used to obtain $\mathbb{E}_{\mathbf{s}[t]}\left[i_{m,n}(p, \mathbf{s}[t])\right]$ in (18).

The receiver maps can also be used to update the stochastic Lagrange multiplier associated with the interference constraint; i.e., $\theta[t]$ in (24). A simple way to update $\theta[t]$, which does not require use of the receiver maps, is to leverage the actual interference notification $i[t]$. In case of system-wide tweets, this amounts to setting $\theta[t+1] = [\theta[t] - \mu_\theta(i^{max} - i[t])]_+$. If such a notification contains errors, $i[t]$ has to be replaced by an unbiased estimate of the actual interference. A more elaborate alternative is to use the receiver maps to *estimate* the actual interference and then update the multiplier as $\theta[t+1] = [\theta[t] - \mu_\theta(i^{max} - \Pr\{i[t] = 1|\mathcal{H}_t\})]_+$. In this case, the interference notification $i[t]$ is first employed to update the maps $\hat{\beta}_{\mathbf{x}}^{(q)}[t|t-1]$. Then, the updated maps $\hat{\beta}_{\mathbf{x}}^{(q)}[t|t]$ for all q and $\mathbf{x}$, and the RA at time t, are used to find $\Pr\{i[t] = 1|\mathcal{H}_t\}$.

The proposed joint RA and receiver map estimation algorithm is tabulated as Algorithm 1.

D. Accounting for PU-SU communication errors

To account for errors in the messages notifying interference, miss-detection and false-alarm events are considered. In particular, let $P_{MD}^{(q)}$ denote the probability of missing an interference tweet sent by PU receiver q, and P_{MD} its counterpart in the setup *(c2)*. Further, let $P_{FA}^{(q)}$ and P_{FA} denote the probability that the messages $i^{(q)}[t] = 1$ and $i[t] = 1$, respectively, were received, but no actual interference was caused. In the following, such probabilities are assumed known.

While the expression for the prediction step in (26) remains the same, the correction step must be adjusted to account for decoding failures and false-interference notifications. The error-aware correction step is first developed for *(c1)*, and subsequently tailored for *(c2)*.

1) Per-PU notification: The main idea is to update the expressions for the variables involved in the correction step in (27) for both $i^{(q)}[t] = 1$ and $i^{(q)}[t] = 0$. Key to this end is to re-write the numerator of (27). Let first define the probabilities

$$P_{\mathbf{x},0}^{(q)}[t] := 1 - \iota_{m,\mathbf{x}}(p_{m^*,n^*}^*, \mathbf{s}[t]) \tag{33}$$

$$P_{\mathbf{x},1}^{(q)}[t] := \iota_{m,\mathbf{x}}(p_{m^*,n^*}^*, \mathbf{s}[t])\,. \tag{34}$$

Clearly, $P_{\mathbf{x},0}^{(q)}[t]$ is the probability of not inflicting interference at time t given the system history $\tilde{\mathcal{H}}_t$, and assuming that $z_{\mathbf{x}}^{(q)}[t] = 1$. Such probabilities are used to define the correction coefficients

$$c_{\mathbf{x}|0}^{(q)} := (1 - P_{FA}^{(q)})P_{\mathbf{x},0}^{(q)}[t] + P_{MD}^{(q)}P_{\mathbf{x},1}^{(q)}[t] \tag{35}$$

$$c_{\mathbf{x}|1}^{(q)} := P_{FA}^{(q)}P_{\mathbf{x},0}^{(q)}[t] + (1 - P_{MD}^{(q)})P_{\mathbf{x},1}^{(q)}[t], \tag{36}$$

which represent the probability of observing $i^q[t] = 0$ and $i^q[t] = 1$, respectively. With these definitions, the correction step for $i^q[t] = o$ is [cf. (27)]

$$\hat{\beta}_{\mathbf{x}}^{(q)}[t|t] = \frac{c_{\mathbf{x}|o}^{(q)}\hat{\beta}_{\mathbf{x}}^{(q)}[t|t-1]}{\sum_{\mathbf{x}' \in \mathcal{G}_{\mathbf{x}}} c_{\mathbf{x}'|o}^{(q)}\hat{\beta}_{\mathbf{x}'}^{(q)}[t|t-1]}\,. \tag{37}$$

Although $P_{MD}^{(q)}$ and $P_{FA}^{(q)}$ have been assumed constant across space, they can be rendered dependent on $\mathbf{x}$. For example, if the Bayesian estimator is implemented at a secondary NC, then the miss-detection probability can be written as $P_{MD}^{(q)} = \Pr\{p^{(q)}h_{\mathbf{x},NC}/\sigma^2 \leq \Gamma\}$, where $h_{\mathbf{x},NC}$ is the PU-to-NC channel, $p^{(q)}$ the power transmitted by PU q, σ^2 the detector noise, and Γ the SINR threshold under which packet decoding is deemed unsuccessful. Clearly, this probability depends on $\mathbf{x}$ and should be written as $P_{MD,\mathbf{x}}^{(q)}$. Accounting for this dependence only requires replacing $P_{MD}^{(q)}$ and $P_{FA}^{(q)}$ with $P_{MD,\mathbf{x}}^{(q)}$ and $P_{FA,\mathbf{x}}^{(q)}$ in (35)-(36).

2) System-wide notification: The main difference compared to the previous case is that the expressions for $P_{\mathbf{x},0}^{(q)}[t]$ and $P_{\mathbf{x},1}^{(q)}[t]$, which account for the probabilities of (not) interfering the PU system at time t given the history $\tilde{\mathcal{H}}_t$ and $z_{\mathbf{x}}^{(q)}[t] = 1$, are more intricate. Specifically, instead of (33) and (34) we have

$$P_{\mathbf{x},0}^{(q)}[t] := \left(1 - \iota_{m,\mathbf{x}}(p_{m^*,n^*}^*, \mathbf{s}[t])\right) \times \prod_{u=1, u\neq q}^{Q} \left(1 - \sum_{\mathbf{x}' \in \mathcal{G}} \iota_{m,\mathbf{x}'}(p_{m^*,n^*}^*[t], \mathbf{s}[t])\hat{\beta}_{\mathbf{x}'}^{(u)}[t|t-1]\right) \tag{38}$$

$$P_{\mathbf{x},1}^{(q)}[t] := 1 - P_{\mathbf{x},0}^{(q)}[t]. \tag{39}$$

Note that, in this case, the above probabilities account for the event of users other than q suffering interference. Once these expressions have been modified, the correction step is implemented by simply substituting (38)-(39) into (35)-(37).

V. Numerical results

Consider the scenario depicted in Fig. 1, where $M = 12$ SU transceivers (marked with green circles) are deployed over an area of 400×400 m and cooperate in routing packets to the sink node U_{12}. One data flow is simulated, and traffic is generated at SUs $\mathcal{N}_S := \{1, 2, 3, 4, 7, 8\}$. A PU transmitter (marked with a purple triangle) communicates with 2 PU receivers (purple rhombus) using a power of 3 dB. The first PU receiver is located at $\mathbf{x}^{(1)} = (x = 250, y = 280)$, static, and it is served by the PU source during the entire simulation interval $t \in [1, 10^4]$. The second PU is located at $\mathbf{x}^{(2)} = (130, 240)$, mobile, with $\phi_{\mathbf{x},\mathbf{x}'}^{(q)}[t] = 0.05\ \forall \mathbf{x}' \in \mathcal{G}_{\mathbf{x}}$, and it is served by

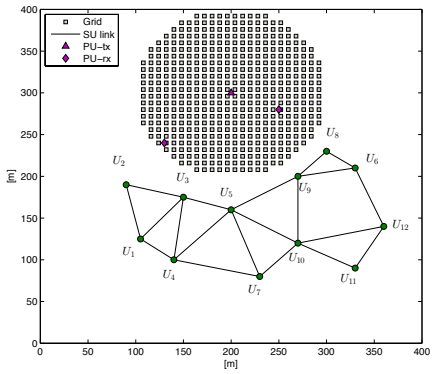

Fig. 1. Simulated scenario.

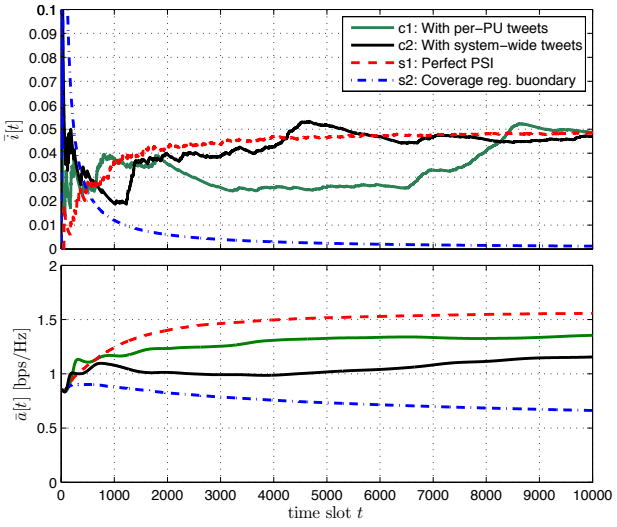

Fig. 2. Convergence of average exogenous rates and average interference.

the PU source only during the interval $[1, 5 \times 10^3]$. The PU system is protected by setting $I = -70$ dB and $i^{\max} = 0.05$. The path loss obeys the model $\gamma_{m,\mathbf{x}} = \|\mathbf{x}_m - \mathbf{x}\|_2^{-3.5}$, while a Rayleigh-distributed small-scale fading is simulated [20].

From the sensing phase, the SU system can acquire an estimate of the PU source location, and of its coverage region (see, e.g., [11]–[13]). The PU coverage region is then discretized using uniformly spaced grid points (marked with gray squares in Fig. 1), each one covering an area of 8×8 m. To assess robustness to model mismatches, it is assumed that: *i)* the SUs have imperfect knowledge of the PU transition probabilities, which are supposed to be $\hat{\phi}^{(q)}_{\mathbf{x},\mathbf{x}'} = 0.01$ for both receivers; and, *ii)* when the system-wide interference notification strategy is adopted (see Section IV-B), the presumed number of PUs is always $Q = 2$, even in the interval $[5 \times 10^3, 10^4]$ where only one PU receiver is present. The multipliers are initialized as $\lambda^k_m[0] = 0.1$, $\pi_m[0] = 0.03$, and $\theta[0] = 40$, while the stepsizes are set to $\mu_\lambda = 0.5$, $\mu_\pi = 0.03$, and $\mu_\theta = 0.3$.

The (performance of the) proposed RA is compared with:
s1) an approach where the beliefs are set to 1 for grid points on the boundary of the PU coverage region [10], [13], [14]; and,
s2) a scheme where perfect PSI (including that of SU-to-PU instantaneous channels) is available.

Clearly, s2 represents an unrealistic scenario, but it serves as a benchmark to assess the performance loss incurred by the lack of full SU-PU coordination. For strategies *s1*-*s2*, $\theta[0]$ is set to 5. A normalized bandwidth $W = 1$ is considered; hence, instantaneous and average rates are expressed in bit/s/Hz. All nodes $\mathcal{N}_S$ generate best-effort traffic ($a^{1,\min}_m = 0$), with a maximum average rate of $a^{1,\max}_m = 1$ bit/s/Hz. Utility and cost functions are $V^k_m = \log_2(a^k_m)$ and $J_m(\bar{p}_m) = \bar{p}^2_m$, respectively, while the coding SINR gap is set to $\kappa_m = 1$ for all U_m.

To highlight the benefits of the PU receiver maps, the total average exogenous rate $\bar{a}[t] := (1/t)\sum_{m\in\mathcal{N}_S}\sum^t_{\tau=1} a^1_m[\tau]$ achieved by the proposed joint RA and receiver map algorithm is depicted in the upper subplot of Fig. 2, and it is compared with the ones obtained by *s1* and *s2*. As expected, higher average rates can be obtained when perfect CSI and PSI are available. On the other hand, the proposed scheme markedly outperforms *s1*, thus justifying the additional complexity required to implement the Bayesian map estimator. The strategy based on a system-wide interference notification leads to moderately worse performance of the SU system compared to the case where per-PU receiver tweets $i^{(q)}[t]$ are broadcasted. This is however not surprising, since the strategy *(c1)* benefits from additional information on the PU system (i.e., the PU receiver that was interfered).

To further corroborate convergence and feasibility of the proposed RA scheme, the running average of the interference $\bar{i}[t] := (1/t)\sum^t_{\tau=1} i[\tau]$ is reported in the lower subplot of Fig. 2. It can be clearly seen that the average interference constraints are enforced when both the proposed and benchmark *s2* algorithms are utilized. On the other hand, *s1* results in an over-conservative approach. This is because the instantaneous probabilities of interference in this case are computed based on the worst-case assumption that receivers are located on the boundary of the PU coverage region, and thus the actual rate of interference is far less than expected.

Pictorially, performance of the receiver localization scheme can be assessed through the maps shown in Fig. 3 (strategy *c1*) and Fig. 4 (strategy *c2*). The value (color) of a point in the map represents the sum of the beliefs $\beta_{\mathbf{x}}[t] := \sum_q \beta^{(q)}_{\mathbf{x}}[t|t]$ at the corresponding grid point $\mathbf{x}$. The chromatic scale uses white for low (belief) values and red for high ones. For *(c1)*, a uniform distribution across the entire PU coverage region is used for both $\beta^{(1)}_{\mathbf{x}}[0|0]$ and $\beta^{(2)}_{\mathbf{x}}[0|0]$. On the other hand, for *(c2)*, a uniform distribution across the south-east and the south-west quarters of the PU coverage region are used for $\beta^{(1)}_{\mathbf{x}}[0|0]$ and $\beta^{(2)}_{\mathbf{x}}[0|0]$, respectively. Maps in Figs. 3 (a), (b), and (c) are acquired at $t = 100$, $t = 1000$, and $t = 6000$, respectively. It can be seen that after 100 time slots, it is already possible to unveil the areas where PU receivers are likely to reside. Clearly, as time goes by, the localization accuracy improves as corroborated by Figs. 3(b) and (c). Remarkably, the PU receiver is perfectly localized in Fig. 3(c).

Recall that only one PU receiver is served by the PU source when $t > 5 \times 10^3$. Indeed, in the setup *(c2)*, the beliefs peak at the actual location of the PU receiver, as shown in Fig. 4(c).

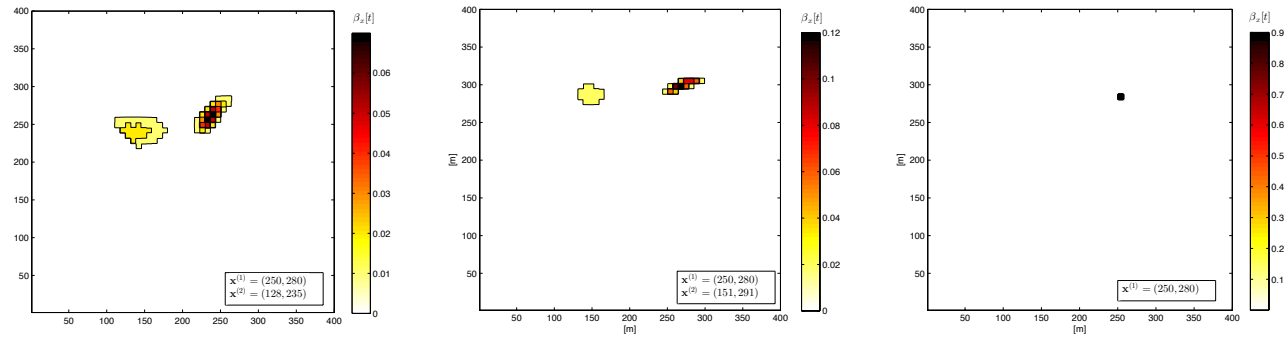

(a) (b) (c)

Fig. 3. Per-PU interference tweet: map of the sum-belief $\beta_{\mathbf{x}}[t]$ per grid point $\mathbf{x}$. (a) $t = 100$; (b) $t = 1000$; (c) $t = 6000$.

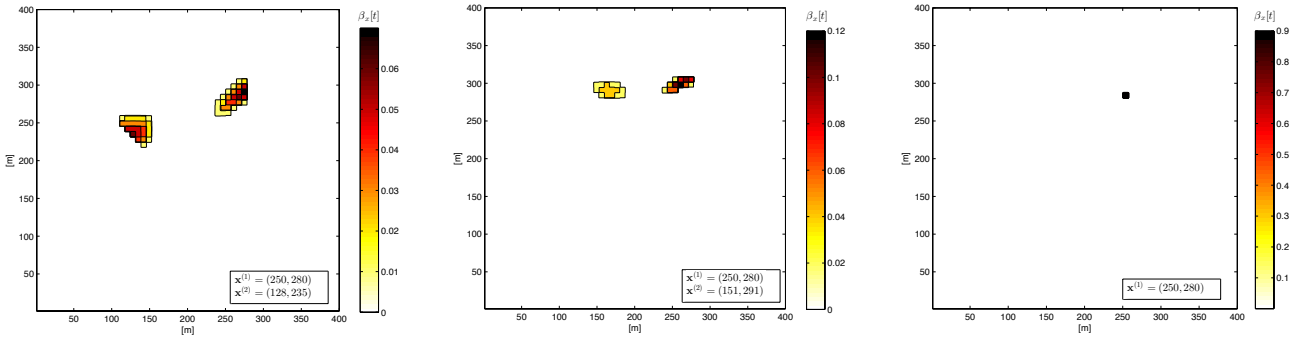

(a) (b) (c)

Fig. 4. System-wide interference notification: map of the sum-belief $\beta_{\mathbf{x}}[t]$ per grid point $\mathbf{x}$. (a) $t = 100$; (b) $t = 1000$; (c) $t = 6000$.

TABLE I
CASE *(c1)*: AVERAGE EXOGENOUS RATES [BIT/S/HZ] FOR DIFFERENT DIMENSIONS OF THE GRID POINT (GP) [METER].

GP	$\bar{a}_1^1$	$\bar{a}_2^1$	$\bar{a}_3^1$	$\bar{a}_4^1$	$\bar{a}_7^1$	$\bar{a}_8^1$	$\sum_i \bar{a}_i^1$
3	0.181	0.138	0.181	0.190	0.289	0.281	1.541
5	0.161	0.130	0.157	0.173	0.304	0.301	1.507
7	0.169	0.137	0.150	0.182	0.299	0.272	1.470
9	0.157	0.150	0.136	0.174	0.298	0.263	1.459
15	0.151	0.149	0.139	0.153	0.250	0.190	1.309

TABLE II
CASE *(c2)*: AVERAGE EXOGENOUS RATES [BIT/S/HZ] FOR DIFFERENT DIMENSIONS OF THE GRID POINT (GP) [METER].

GP	$\bar{a}_1^1$	$\bar{a}_2^1$	$\bar{a}_3^1$	$\bar{a}_4^1$	$\bar{a}_7^1$	$\bar{a}_8^1$	$\sum_i \bar{a}_i^1$
3	0.174	0.127	0.154	0.182	0.314	0.324	1.275
5	0.176	0.157	0.163	0.186	0.296	0.273	1.248
7	0.161	0.168	0.167	0.180	0.284	0.243	1.204
9	0.167	0.148	0.175	0.177	0.313	0.260	1.240
15	0.159	0.143	0.182	0.169	0.265	0.268	1.187

The numerical results reveal that the two beliefs $\beta_{\mathbf{x}}^{(1)}[t|t]$ and $\beta_{\mathbf{x}}^{(2)}[t|t]$ are (approximately) the same for all $\mathbf{x}$, thus indicating that just an upper bound on Q is sufficient to carry out the receiver localization task.

Resolution of the grid $\mathcal{G}$ clearly affects the receiver localization accuracy; at the expense of an higher computational burden, finer grids allow the SU system to pinpoint the receivers' locations with higher accuracy [11]. This, is turn, influences also the RA performance, as verified by Table I. Specifically, Table I reports the running average rates $\bar{a}_i^1 := (1/t) \sum_\tau a_i^1[\tau]$, $\forall\, i \in \mathcal{N}_S$ at time $t = 5 \times 10^3$, along with the overall rate $\bar{a}^1 := \sum_{i \in \mathcal{N}_S} \bar{a}_i^1$. A per-PU interference notification strategy is implemented. It can be seen that the total rate $\bar{a}^1$ increases as the grid becomes more dense. Users U_7 and U_8 achieve higher traffic rates, since they are just two hops away from the destination; this can be observed also in Table III, where the same results are reported for benchmark *s2*. Remarkably, when each grid point covers a 3×3 m area, the gap between the overall exogenous rates obtained with the proposed scheme, and the one with perfect CSI and PSI is of just 0.001 bit/s/Hz. Further, thanks to the receiver maps, U_8 can achieve high data rates (compared to the other SU sources) even though it is geographically close to the PU system. On the other hand, U_8 achieves an average rate one order of magnitude smaller by using the RA scheme *s1*, as shown in Table III. The average exogenous rates achieved when tweets $i[t]$ are

TABLE III
CASES *(s1)* AND *(s2)*: AVERAGE EXOGENOUS RATES [BIT/S/HZ].

	$\bar{a}_1^1$	$\bar{a}_2^1$	$\bar{a}_3^1$	$\bar{a}_4^1$	$\bar{a}_7^1$	$\bar{a}_8^1$	$\sum_i \bar{a}_i^1$
s1	0.128	0.077	0.059	0.139	0.256	0.066	0.725
s2	0.184	0.163	0.206	0.203	0.317	0.469	1.542

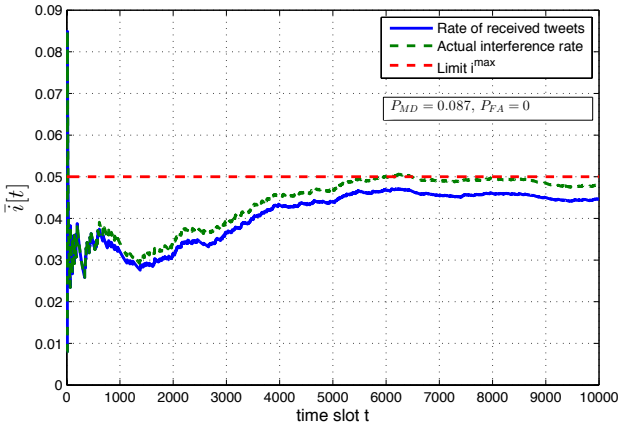

Fig. 5. Average interference rate with communication outages.

exchanged between the systems are reported in Table II. Again, SUs attain higher rates by using a fine-grained discretization of the PU coverage region. Strategy *(c2)* leads to moderately worse performance of the SU system, and the gap with the overall rates achieved using per-PU receiver tweets $i^{(q)}[t]$ is on the same order in all the cases tested.

Next, the case where the secondary system does not correctly decode all the interference tweets is tested. Suppose that the sink node U_{12} acts as an NC for the secondary system, and assume that strategy *(c2)* is employed. The probability of outage on the communication link between the PU transmitter and SU U_{12} is set to $P_{MD} = 0.087$, which corresponds to the probability that the instantaneous SINR at U_{12} stays below a given threshold [20]. Further, assume that each grid point covers an area of 8×8 m. The trajectory of the cumulative moving average of the interference is shown Fig. 5. Specifically, the cumulative moving average of both the actual interference and the interference tweets received are plotted. As expected, for $t > 6000$ the rate of correctly received tweets floors at a level slightly lower than $i^{\max}$. Indeed, the actual interference rate levels off at $i^{\max}$, thus protecting the PU system from excessive interference despite communication errors.

VI. Concluding Remarks

Dynamic cross-layer resource allocation and user localization algorithms for an underlay multi-hop cognitive radio network were designed. A robust recursive Bayesian approach was developed to estimate (and track) the unknown location of the PU receivers. The inputs of the estimator were the (past and current) power transmitted by the secondary system, and a binary interference notification (tweet) broadcasted by the primary system. The schemes were found robust to errors on the observations and accounted for PU mobility. The estimated maps and the remaining CSI serve as input of a cross-layer optimization. In particular, the resource allocation schemes were obtained as the solution of a constrained network-utility maximization that optimized performance of the secondary network and accounted for the distinctive features of the cognitive setup, including a constraint that limited the long-term probability of interfering the primary receivers. The optimal solution dictated how to adapt the resources at different layers as a function of the perfect CSI of the SU-to-SU links and the uncertain CSI of the SU-to-PU links. Numerical results validated the novel approach and confirmed that such a minimal feedback suffices to accurately estimate (and track) the location of PU receivers.

Appendix: Proof of Propositions 3 and 4

Rearranging the terms of $\mathcal{L}(\mathcal{Y}, \mathbf{d}^*)$ and isolating those dependent on $\{r^k_{m,n}[t]\}$, $\{w_{m,n}[t]\}$, and $\{p_{m,n}[t]\}$, we have that $\mathbb{E}_{\mathbf{g},\mathbf{s}}[\sum_{(m,n)\in\mathcal{E}}[\sum_k r^k_{n,m}\lambda^{k*}_{m,n} - \pi^*_m w_{m,n}p_{m,n} - \theta^* w_{m,n} i_{m,n}(p_{m,n})]]$. Clearly, the latter is separable per-fading state. Hence, maximizing the Lagrangian amounts to solving, per fading state, the problem

$$\max_{\{r^k_{m,n}, w_{m,n}, p_{m,n}\}} \sum_{(m,n)\in\mathcal{E}} \Big[\sum_k r^k_{n,m}\lambda^{k*}_{m,n} - \pi^*_m w_{m,n}p_{m,n} - \theta^* w_{m,n}\mathbb{E}_{\mathbf{s}[t]}[i_{m,n}(p_{m,n})]\Big] \quad (40a)$$

$$\text{s.to} \sum_k r^k_{n,m} \le w_{m,n} C_{m,n}(\mathbf{g}[t], p_{m,n}), \forall (m,n) \in \mathcal{E} \quad (40b)$$

$$\sum_{(m,n)\in\mathcal{E}} w_{m,n} \le 1,\ p_{m,n} \in [0, p^{\max}_m],\ w_{m,n} \in [0,1], \quad (40c)$$

where the constraints not dualized have been written explicitly.

Consider first solving (40) w.r.t. $\{r^k_{m,n}\}$. Per link (m,n), and for any given value of $w_{m,n}$ and $p_{m,n}$, rates $r^{k*}_{m,n} \ge 0$ are obtained by maximizing a linear function over a simplex. Thus, the optimal arguments $r^{k*}_{m,n}$ will lie on the boundary of the constraints. Recall that $\lambda^*_{m,n} = \max_k \lambda^{k*}_{m,n}$ and define $\mathcal{K}_{m,n} := \{k : \lambda^*_{m,n} = \lambda^{k*}_{m,n}\}$. Then, it is straightforward to show that: i) if $\lambda^{k*}_{m,n} \le 0$, then $r^{k*}_{m,n} = 0$ for all k; and if $\lambda^{k*}_{m,n} > 0$, then $r^{k*}_{m,n} = 0$ for $k \notin \mathcal{K}_{m,n}$ and $\sum_{k\in\mathcal{K}_{m,n}} r^k_{n,m} = w_{m,n}C_{m,n}(\mathbf{g}[t], p_{m,n})$. This is in fact, the main result in Proposition 4. As a special case, when all weights $\lambda^{k*}_{m,n}$ are different, one has the "winner-takes-all" solution (21).

After substituting $\{r^{k*}_{m,n}\}$ into (40a), one can drop constraint (40b) and replace $\sum_k r^k_{n,m}\lambda^{k*}_{m,n}$ with $\sum_{\mathcal{K}_{m,n}} r^k_{n,m}\lambda^*_{m,n}$ and the latter with $w_{m,n}C_{m,n}(\mathbf{g}[t], p_{m,n})\lambda^*_{m,n}$. Hence, the optimum $\{w^*_{m,n}\}$, and $\{p^*_{m,n}\}$ are found by solving

$$\max_{\{w_{m,n}, p_{m,n}\}} \sum_{(m,n)\in\mathcal{E}} \Big[w_{m,n}C_{m,n}(\mathbf{g}[t], p_{m,n})\lambda^*_{m,n} - \pi^*_m w_{m,n}p_{m,n} - \theta^* w_{m,n}\mathbb{E}_{\mathbf{s}[t]}[i_{m,n}(p_{m,n})]\Big] \quad (41a)$$

$$\text{s.to} \sum_{(m,n)\in\mathcal{E}} w_{m,n} \le 1\,,\ p_{m,n} \in [0, p^{\max}_m],\ w_{m,n} \in [0,1]. \quad (41b)$$

Recall that the definition of the link-quality indicator is [cf. (17)] $\varphi_{m,n}(\mathbf{g}[t], p_{m,n}) = \lambda^*_{m,n} C_{m,n}(\mathbf{g}[t], p_{m,n}) - \pi^*_m w_{m,n}p_{m,n} - \theta^* w_{m,n}\mathbb{E}_{\mathbf{s}[t]}[i_{m,n}(p_{m,n})]$. Then, (41a) can be rewritten as

$$\max_{\{w_{m,n}, p_{m,n}\}} \sum_{(m,n)\in\mathcal{E}} w_{m,n}\varphi_{m,n}(\mathbf{g}[t], p_{m,n})\,. \quad (42)$$

It is then clear that: i) for any value of $w_{m,n}$, the optimal power can be found separately as $p^*_{m,n} = \arg\max_{p_{m,n}}$

$\varphi_{m,n}(\mathbf{g}[t], p_{m,n})$ s. to $p_{m,n} \in [0, p_m^{\max}]$; and ii) the optimal scheduling coefficients are found as $w_{m,n}^* = \arg\max_{\{w_{m,n}\}} \sum_{(m,n)\in\mathcal{E}} w_{m,n}\varphi_{m,n}(\mathbf{g}[t], p_{m,n}^*)$ s. to $w_{m,n} \in [0,1]$ and $\sum_{(m,n)\in\mathcal{E}} w_{m,n} \leq 1$. Clearly, this is a linear program and its solution lies on the boundary of the constraints. Specifically, $w_{m,n}^* = 0$ unless $(m,n) = \arg\max_{m',n'} \varphi_{m',n'}(\mathbf{g}[t], p_{m',n'}^*)$. These are precisely the results in Proposition 3.

REFERENCES

[1] Q. Zhao and B. M. Sadler, "A survey of dynamic spectrum access," *IEEE Sig. Proc. Mag.*, vol. 24, no. 3, pp. 79–89, May 2007.

[2] A. Ghasemi and E. S. Sousa, "Fundamental limits of spectrum-sharing in fading environments," *IEEE Trans. Wireless Commun.*, vol. 6, no. 2, pp. 649–658, Feb. 2007.

[3] Y. Chen, G. Yu, Z. Zhang, H.-H. Chen, and P. Qiu, "On cognitive radio networks with opportunistic power control strategies in fading channels," *IEEE Trans. Wireless Commun.*, vol. 7, no. 7, pp. 2752–2761, Jul. 2008.

[4] R. Zhang, "On peak versus average interference power constraints for protecting primary users in cognitive radio networks," *IEEE Trans. Wireless Commun.*, vol. 8, no. 4, pp. 2112–2120, Apr. 2009.

[5] S. Huang, X. Liu, and Z. Ding, "Decentralized cognitive radio control based on inference from primary link control information," *IEEE J. Sel. Areas Commun.*, vol. 29, pp. 394–406, Feb. 2011.

[6] X. Kang, Y.-C. Liang, A. Nallanathan, H. K. Garg, and R. Zhang, "Optimal power allocation for fading channels in cognitive radio networks: Ergodic capacity and outage capacity," *IEEE Trans. Wireless Commun.*, vol. 8, no. 2, pp. 940–950, Feb. 2009.

[7] X. Wang, "Joint sensing-channel selection and power control for cognitive radios," *IEEE Trans. Wireless Commun.*, vol. 10, no. 3, pp. 958–967, Mar. 2011.

[8] X. Gong, S. Vorobyov, and C. Tellambura, "Optimal bandwidth and power allocation for sum ergodic capacity under fading channels in cognitive radio networks," *IEEE Trans. Sig. Proc.*, vol. 59, no. 4, pp. 1814–1826, Apr. 2011.

[9] A. G. Marques, L. M. Lopez-Ramos, G. B. Giannakis, and J. Ramos, "Resource allocation for interweave and underlay cognitive radios under probability-of-interference constraints," *IEEE J. Sel. Areas Commun.*, vol. 30, no. 10, pp. 1922–1933, Nov. 2012.

[10] E. Dall'Anese, S.-J. Kim, G. B. Giannakis, and S. Pupolin, "Power control for cognitive radio networks under channel uncertainty," *IEEE Trans. Wireless Commun.*, vol. 10, no. 10, pp. 3541–3551, Dec. 2011.

[11] E. Dall'Anese, J. A. Bazerque, and G. B. Giannakis, "Group sparse Lasso for cognitive network sensing robust to model uncertainties and outliers," *Elsevier Phy. Commun.*, vol. 5, no. 2, pp. 161–172, Jun. 2012.

[12] J. Wang, P. Urriza, Y. Han, and D. Čabrić, "Weighted centroid algorithm for estimating primary user location: Theoretical analysis and distributed implementation," *IEEE Trans. Wireless Commun.*, vol. 10, no. 10, pp. 3403–3413, Oct. 2011.

[13] B. Mark and A. Nasif, "Estimation of maximum interference-free power level for opportunistic spectrum access," *IEEE Trans. Wireless Commun.*, vol. 8, no. 5, pp. 2505–2513, May 2009.

[14] E. Dall'Anese and G. B. Giannakis, "Statistical routing for multihop wireless cognitive networks," *IEEE J. Sel. Areas Commun.*, vol. 30, no. 10, pp. 1983–1993, Nov. 2012.

[15] Y. Ho and R. Lee, "A Bayesian approach to problems in stochastic estimation and control," *IEEE Trans. Auto. Contr.*, vol. 9, no. 4, pp. 333–339, Oct. 1964.

[16] V. Cevher, P. Boufounos, R. G. Baraniuk, A. C. Gilbert, and M. J. Strauss, "Near-optimal Bayesian localization via incoherence and sparsity," in *Intl. Conf. on Info. Proc. in Sensor Netw.*, San Francisco, CA, Apr. 2009, pp. 205–216.

[17] N. Patwari and A. O. Hero III, "Using proximity and quantized RSS for sensor localization in wireless networks," in *2nd ACM Intl. Conf. on Wireless Sensor Netw. and App.*, 2003, pp. 20–29.

[18] K. Eswaran, M. Gastpar, and K. Ramchandran, "Bits through ARQs: Spectrum sharing with a primary packet system," in *in Proc. of IEEE Intl. Symp. on Info. Theory*, Nice, France, Jun. 2007, see also: `http://arxiv.org/pdf/0806.1549.pdf`.

[19] A. G. Marques, L. M. Lopez-Ramos, G. B. Giannakis, J. Ramos, and A. Caamano, "Resource allocation for interweave and underlay cognitive radios under probability-of-interference constraints," *IEEE Trans. Veh. Technol.*, vol. 61, no. 6, pp. 2789 – 2807, Jul. 2012.

[20] A. Goldsmith, *Wireless communications*. Cambridge University Press, 2005.

[21] E. Dall'Anese, S.-J. Kim, and G. B. Giannakis, "Channel gain map tracking via distributed Kriging," *IEEE Trans. Veh. Technol.*, vol. 60, no. 3, pp. 1205–1211, Mar. 2011.

[22] L. Georgiadis, M. J. Neely, and L. Tassiulas, "Resource allocation and cross-layer control in wireless networks," *Found. Trends in Networking*, vol. 1, no. 1, pp. 1–144, 2006.

[23] Y.-J. Chang, F.-T. Chien, and C.-C. Kuo, "Cross-layer QoS analysis of opportunistic OFDM-TDMA and OFDMA networks," *IEEE J. Sel. Areas Commun.*, vol. 25, no. 4, pp. 657–666, May 2007.

[24] T. Yoo and A. Goldsmith, "Capacity and power allocation for fading mimo channels with channel estimation error," *IEEE Trans. Info. Theory*, vol. 52, no. 5, pp. 2203–2214, May 2006.

[25] A. Ribeiro and G. B. Giannakis, "Separation principles in wireless networking," *IEEE Trans. Info. Theory*, vol. 56, no. 9, pp. 4488–4505, Sep. 2010.

[26] L. Chen, S. H. Low, M. Chiang, and J. C. Doyle, "Cross-layer congestion control, routing and scheduling design in ad hoc wireless networks," in *Proc. of IEEE INFOCOM*, Barcelona, Spain, Apr. 2006.

[27] X. Lin and N. B. Shroff, "The impact of imperfect scheduling on cross-layer congestion control in wireless networks," *IEEE/ACM Trans. on Netw.*, vol. 14, no. 2, pp. 302–315, Apr. 2006.

[28] A. G. Marques, , X. Wang, and G. B. Giannakis, "Dynamic resource management for cognitive radios using limited-rate feedback," *IEEE Trans. Sig. Proc.*, vol. 57, no. 9, pp. 3651–3666, Sep. 2009.

[29] A. Ribeiro, "Ergodic stochastic optimization algorithms for wireless communication and networking," *IEEE Trans. Sig. Proc.*, vol. 58, no. 12, pp. 6369–6386, Dec. 2010.

[30] D. Bertsekas, A. Nedic, and A. E. Ozdaglar, *Convex Analysis and Optimization*. Athena Scientic, 2003.